
CHAPTER 0: PRELIMINARIES

A. LEARNING OBJECTIVES

- To learn the terminology and notation of nuclear physics
- To understand the physical reasoning behind models of the nucleus
- To understand processes such as radioactive decay
- Become aware of applications of nuclear physics in science, technology, and medicine
- Learn to solve nuclear problems through assignments and present clear cogent arguments

B. SYLLABUS

Chapter 0: Introduction and preliminaries

Chapter 1: Nuclear properties and abundance

Chapter 2: The inter-nucleon potential

Chapter 3: Models of the nucleus

- Liquid drop model
- Shell Model
- Collective model

Chapter 4: Nuclear Decay processes

- Alpha decay
- Beta decay
- Gamma decay

Chapter 5: Fission and Fusion

- Fission
- Fusion

C. UNITS

- In SI units the energy is in Joules (J). Conversion to electronvolts (eV) is simply by dividing by $e = 1.602 \times 10^{-19}$. Often energies are quoted in $\text{MeV} = 1.6 \times 10^{-13} \text{ J}$.
- Masses are often given in MeV units, which are units of energy. The atomic mass unit, $u = 931.5 \text{ MeV}$ and u is defined using $^{12}\text{C} = 12.0000u$ (A neutral carbon atom in the ground state). This is because mass and energy are interchangeable and linked via Einstein's famous equation $E = mc^2$ where m is the mass and c is the speed of light.

- Distances are often quoted in femtometres, $1 \text{ fm} = 10^{-15} \text{ m}$.
- We will often use the relativistic relationship between mass, momentum, and energy

$$E^2 = p^2c^2 + m_0^2c^4$$

where E is the total energy (mass plus kinetic), p is the momentum and m_0 is the rest mass, whilst c is the speed of light.

D. THE IMPORTANCE OF NUCLEAR PHYSICS

We will cover several applications as we go through the chapters. For now, we can note the following examples of how important nuclear physics is.

- Radioactivity warms the core of the Earth. Without it, Lord Kelvin estimated that the Earth would cool in ~ 100 million years. There would then be no magneto-hydrodynamic motion in the core generating a B field that protects us from the solar wind.
- Hans Bethe a long time ago showed that nuclear fusion powers the stars. Nuclear astrophysics is an important way to understand the structure and evolution of stars.
- Radiotherapy and diagnostics such as PET and MRI scans depend on our understanding of nuclear physics. Nuclear physics is thus important in the treatment of cancer and other diseases.
- Nuclear power from both fission (existing) and fusion (perhaps later) are potentially important energy generation methods that do not generate CO_2 emissions as fossil fuels do.
- The internucleon force that we will learn about is a manifestation of the strong force, which is one of the four fundamental forces. Nuclear physics is part way to fundamental particle physics and is a, still not fully understood, and an active research area
- Carbon dating and other radioactive decay dating methods are very useful in geology and palaeontology as we shall see in the lectures.

E. SUGGESTED READING

Eisberg and Resnick: Quantum Physics of Atoms, Molecules, Solids, Nuclei and Particles (Wiley 2nd Edition). Chapter 15 in entirety, Chapter 16 sections 16-1,16-2,16-3,16-5,16-9 and 16-10

KS Krane: Introductory Nuclear Physics (Wiley). Chapter 1, whole chapter, Chapter 3, Whole chapter, Chapter 4, introduction, and sections 4.1 and 4.4, Chapter 5, sections 5.1 and 5.2, Chapter 7 up to section 7.6 inclusive, chapter 8 section 8.1-8.4, chapter 9 section 9.1, Chapter 13, sections 13.1-13.3 and sections 13.5,13.6, chapter 14, chapters 19 and 20.

CHAPTER 1: OBSERVATION OF NUCLEAR PROPERTIES

Composition and notation:

Nuclei are made up of N neutrons and Z protons to have atomic mass number $A = N + Z$. The name *nucleon* is often used collectively for either a proton or neutron. At low Z we have $N \sim Z$. At high Z we have $N > Z$ such that $Z/A \sim 2/5$. (See figure 1.1 below).

For a given element, the chemical properties, and hence name, of the element are decided by the number of protons, Z . The number of neutrons, N only has a very weak effect on these properties and an element can have several different *isotopes*, where the nuclei have the same Z but different N . The full notation is given by:

$${}^A_Z X_N$$

where, X is the chemical symbol. Since the chemical element name depends on Z , it is usual to drop the Z and N subscripts since there are fully determined from the chemical symbol and the atomic mass number, A . So, for example, we have ${}^{27}\text{Al}$ and ${}^{235}\text{U}$ as examples of isotopes.

The occurrence of stable nuclei is related to the oddness or evenness of Z and N as seen in table 1.1 below.

Table 1.1 Occurrence of nuclei depending on oddness or evenness of protons and neutron numbers

| A | N | Z | Stable Nuclei |
|------|------|------|---------------|
| Even | Even | Even | 166 |
| | Odd | Odd | 8 |
| Odd | Even | Odd | 57 |
| | Odd | Even | 53 |

So, we can see that odd-odd nuclei that are stable are in fact quite rare. We will try to understand this during this course.

We also note that, at higher atomic mass, A , the ratio of protons to neutrons decreases. This means that at low atomic number, we have $Z \sim 0.5A$ and the numbers are roughly equal. Think, for example of oxygen, where we have ${}^{16}\text{O}$ as the most stable isotope with 8 neutrons and 8 protons. However, also think about ${}^{208}\text{Pb}$ which has $Z=82$ but $N=126$, so $Z \sim 0.4A$. We can see this phenomenon illustrated in the Segré chart of figure 1.1.

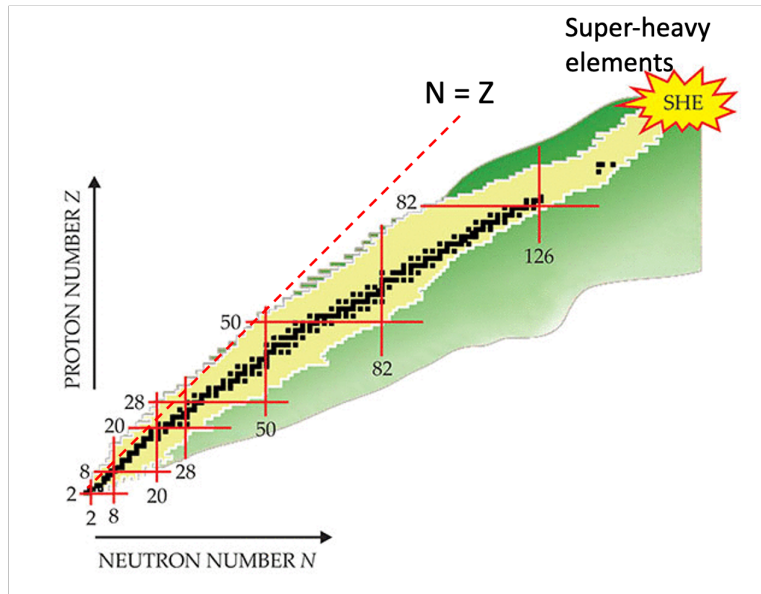


Figure 1.1 Segré chart of nuclei. We see the stable elements (black squares) veer away from $N=Z$ as we increase atomic mass, A . The numbers 2, 8, 20 etc are "magic numbers" that confer particular stability as discussed in Chapter 3.

Abundance of nuclei

Not all nuclei are as common as each other. The observations made in astrophysics and geology have led to an understanding that the abundance of elements is as shown in figure 1.2 below.

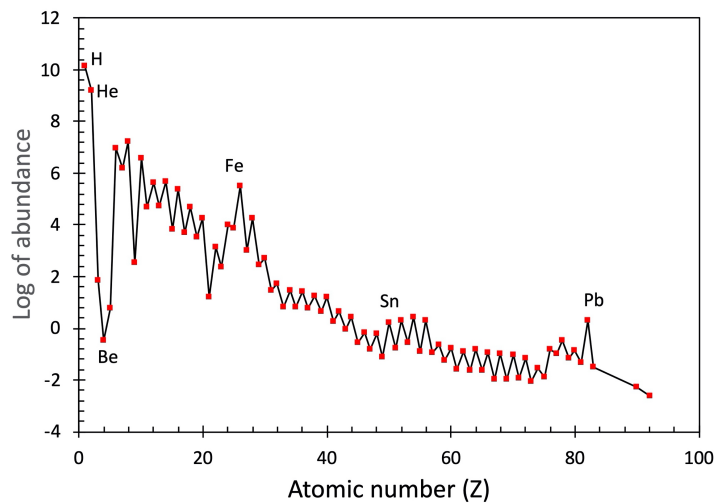


Figure 1.2 Abundance of elements in the universe. The scale is normalised $Si=10^6$.

We can see that hydrogen and helium are by far the most common. There is a dip before abundance rises at carbon and we see oscillations and other peaks. A key goal of nuclear astrophysics is to understand how this distribution of abundance came about.

Nuclei have spin and parity:

In nuclear physics, there is a slight difference in naming compared to atomic physics. If we take the total angular momentum of a nucleus,

$$\mathbf{J} = \mathbf{L} + \mathbf{S} \quad (1.2)$$

Then, this is called the *nuclear spin*, which can be a little confusing, but we can try to help by referring to \mathbf{S} as intrinsic spin. This is the same as electron spin. For both nucleon types, the magnitude is $s = \frac{1}{2}$, where the lower case refers to a single particle. We will note later that for all even-even nuclei the ground state is $\mathbf{J} = 0$. The spins of both nucleons evidently *pair off* to cancel each other and this is due to being energetically advantageous in a phenomenon that is called the *pairing energy* or sometimes *pairing force*. It is a complex phenomenon that helps explain why there are so many even-even nuclei with all nucleons paired off.

We can note that, if a nucleus has odd integer A , then it will have a *spare* proton or neutron and since they are (intrinsic) spin- $\frac{1}{2}$ particles, the nucleus will have a half-integer spin. For even A , we have integer spin, and this is generally true, even for odd-odd nuclei which have both a spare neutron *and* proton. We note that for a nuclear level with spin J , we have $2J+1$ states (this is the number of distinct z components, J_z).

The nuclei also have property called *parity*. This is given by $P = (-1)^L$ where L is the orbital angular momentum quantum number. Parity is a property of the wave-functions that derives from the fact that for $L = \text{even}$ ($P = +1$) wavefunctions, we have the property

$$\psi(r) = \psi(-r) \quad (1.3)$$

whilst for $L = \text{odd}$ ($P = -1$) wavefunctions, we have

$$\psi(r) = -\psi(-r) \quad (1.4)$$

This has some consequences for transitions between nuclear states that we will explore a little further on. Nuclear states are usually therefore denoted by spin and parity J^P . For example, all even-even nuclei have a ground state $J^P = 0^+$, meaning that there is no net angular momentum and thus $L=0$ and so $P=+1$. We will discuss in chapter 3, why this is so. For ^{27}Al which has 14 neutrons but an odd number (13) of protons, we have $J^P = \frac{5}{2}^+$, meaning that the ground state of the nucleus has net angular momentum and spin and that $L = \text{even}$.

Nuclei have magnetic dipole and electric quadrupole moments

All nucleons, including the neutrons, contain charged particles (*quarks*) within them. They have charges that add up to $+e$ for the proton and 0 for the neutron. The orbital motion of these moving charges, for both protons and neutrons, leads to an intrinsic B-field that interacts with external B fields and can be described by a *magnetic dipole moment*

$$\mu_{\text{nuclear}} = g\mathbf{J}\mu_n \quad (1.5)$$

where \mathbf{J} is the nuclear spin and g is a factor like the Landé g -factor in the atomic Zeeman effect. The nuclear magneton is defined by

$$\mu_n = \frac{e\hbar}{2M_P} \approx 10^{-3} \mu_{Bohr} \quad (1.6)$$

The effect of this magnetic moment can be seen in the interaction of the nucleus with the B-field of the atomic electrons to give hyper-fine structure in atomic spectra, which is used as a way of determining the nuclear magnetic dipole. As we see, from equation 1.6, the “nuclear magneton” is about a thousand times smaller than the “Bohr magneton” of atomic physics. For even A values, we have $\mathbf{J} = 0$ and thus zero magnetic dipole. The proton and neutron both have finite magnetic dipoles individually, with

$$\begin{aligned} \mu_{neutron} &= -1.91\mu_n \\ \mu_{proton} &= +2.79\mu_n \end{aligned} \quad (1.7)$$

These values are a result of both particles being in fact made up of three quarks, which carry charge. As noted above, the neutron can have a finite magnetic moment even though it is overall neutral.

The electric quadrupole arises from the fact that the charge in the nucleus is not distributed in a spherically symmetric way. The existence of an electric quadrupole shows some nuclei are not spherical but oblate or prolate. In figure 1.2 we give a simple explanation of what electric dipole and quadrupoles are.

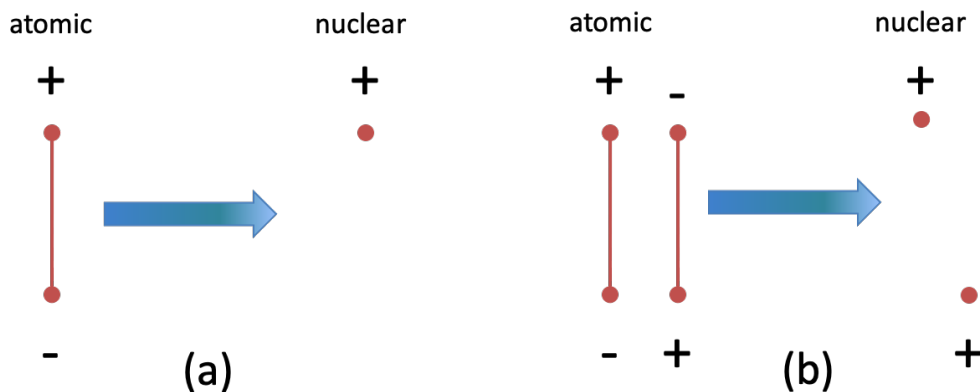


Figure 1.3 (a) Simple illustration of what an electric dipole is. For an atom, we have both positive and negative charges and so can have an electric dipole moment if they are not centred symmetrically about zero. For a nucleus with only positive charges, this does not work, and we don't have an electric dipole moment. We can see this by removing the negative charges as in the figure. (b) Simple illustration of an electric quadrupole. For a nucleus, we can see, that by removing negative charges, we still get a distribution that does not look like a central symmetric charge, and we do have a quadrupole moment.

If a nucleus does not have a spherical shape, then it will have a so-called *quadrupole moment*. In brief it is defined formally by

$$Q_0 = \int \rho(r)(3z^2 - r^2)dv \quad (1.8)$$

Where $\rho(r)$ is the charge density distribution as a function of position r . Note that the position r has components in the x , y and z directions and $r^2 = x^2 + y^2 + z^2$. If the distribution is isotropic then since the averages in all three directions average out to the same values, then so do r^2 and $3z^2$ and the quadrupole moment is zero. Figure 1.3 shows how the shape of the nucleus can change the quadrupole moment. More complex nuclear distortions can occur due to nuclear vibrations, leading to higher order moments, such as octupole moments, but this is beyond our remit for now.

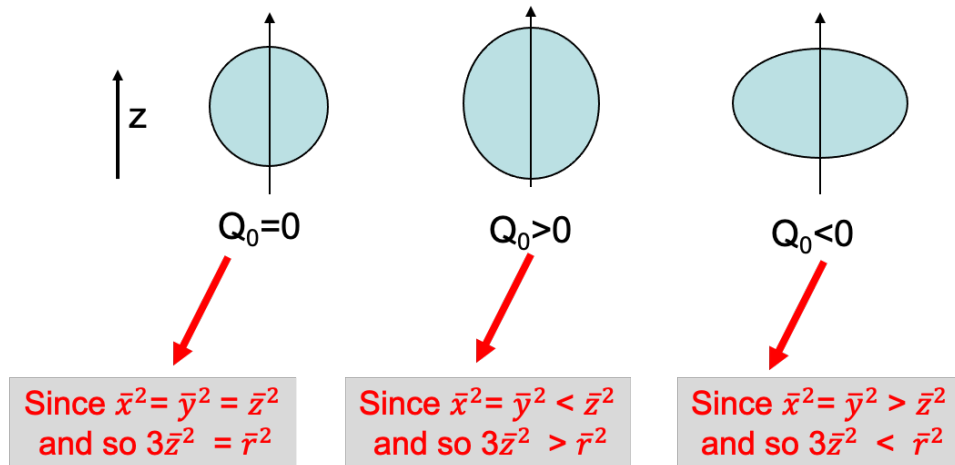


Figure 1.3 A simple illustration of how the shape of a nucleus changes the quadrupole moment, which can be positive or negative. A prolate shape gives $Q > 0$ whilst an oblate shape gives $Q < 0$.

The mass of atoms and nuclei

This mass of an atom is overwhelmingly made up of the mass of its nucleons. However, it is common to use the *atomic mass* as this is very accurately measured. However, the mass is less than the sum of its components.

$$M_{atomic} < ZM_p + NM_n + ZM_e \quad (1.9)$$

The difference is due to the binding energy. Recall that $E = mc^2$, so we can see that the atom at rest can be thought of as having mass energy only, no kinetic energy. If we add just enough energy to separate out all the component particles so that they are at rest but far enough from each other not to interact, then their total mass energy must be the initial mass energy plus the extra energy needed for separation- this extra is the *binding energy*. So that we can say, if we define binding energy, E_B as a positive number,

$$E_B = (ZM_p + NM_n + ZM_e) - M_{atomic} \quad (1.10)$$

Figure 1.4 shows the binding energy curve as a function of atomic mass number. We see there is a maximum stability (i.e., most binding energy per nucleon) at about $A=60$. We shall develop an understanding of this curve via the liquid drop model in the next sections.

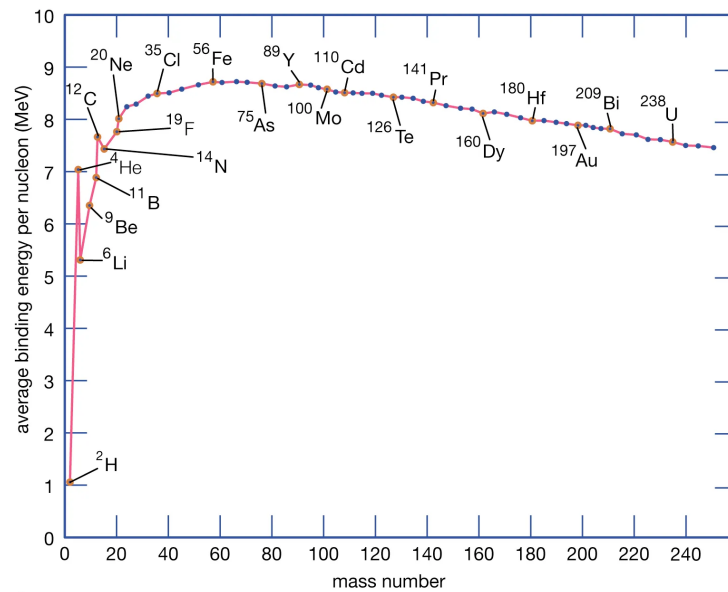


Figure 1.4 Binding energy curve. Note how the binding per nucleon peaks at around 8.8 MeV per nucleon at $A \sim 60$. The most stable atomic mass is around here. We shall see how this curve impacts on nuclear stability in later chapters.

Atomic masses can be measured a quite precisely with careful use of mass spectrometers. Below is a selection of masses in the atomic mass unit:

$$\begin{aligned} \text{Mass } ^{12}\text{C} &= 12.0000\text{u (definition of u)} \\ M_p &= 1.00727647\text{u} \\ M_n &= 1.00866501\text{u} \end{aligned}$$

where the atomic mass unit, u in MeV (energy) units is

$$1 \text{ u}c^2 = 931.502 \text{ MeV}$$

and the mass of ^{12}C neutral atom, as noted above, is defined as exactly 12 atomic mass units. Note that the proton and neutron masses (M_p and M_n) are similar but not identical. This will become important in discussion of β -decay. The masses are often expressed in MeV and this is shorthand for the mass-energy, which of course is given by mc^2 . An important thing to note is that it is the atomic mass that is usually measured precisely. For example, in the back of Krane you can see the masses of all isotopes to several decimal places.

Nuclear size and density

There is more than one way in which the size of a nucleus is determined. We can consider one way that uses fast electron diffraction. Consider a fast electron. It has a wave property such that; $p = h/\lambda$, where p is the momentum. We know from level 1 optics that a circular object in the way of a plane wave (usually a laser) will form a diffraction pattern (Airy rings). The minima are at a scatter angle given by:

$$\sin(\theta) = \frac{1.22\lambda}{D} \quad (1.11)$$

where D is the size of the object. Look at figure 1.5. You can see electrons diffracted from ^{16}O nuclei with a first minimum at $\sim 50^\circ$ scatter angle, when electrons of 374.5 MeV are used. (see figure 15-5 in Eisberg and Resnick for another example). Now remember

$$E^2 = p^2c^2 + m_0^2c^4 \quad (1.12)$$

In our case, $E \gg m_0c^2$ and we can approximate $E \sim pc$. We can then use the de Broglie relation to get $\lambda \sim 3.3$ fm and thus D , the size of the nucleus is ~ 5.3 fm. Now the nucleus is not a disk but a 3-D object, and closer analysis shows that the charge distribution of protons can be approximated by

$$\rho(r) = \frac{\rho(0)}{1 + e^{((r-R_0)/a)}} \quad (1.13)$$

where we have,

$$R_0 \sim 1.2A^{1/3} \text{ fm} \quad (1.14)$$

and a ~ 0.55 fm. This means that typically a large nucleus has a flat density in the middle. As we can see in figure 1.6, there is a region where the density falls from 90% of the peak to 10%. The width of this layer is constant at about 2.4 fm, not depending on the atomic mass number, A .

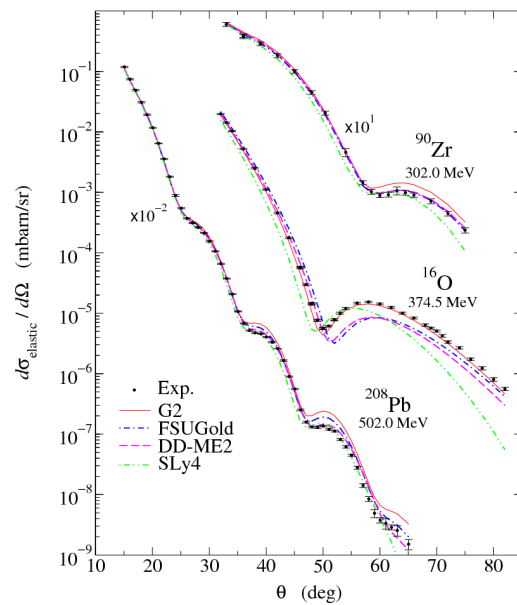


Figure.1.5 This figure shows minima in the scatter of electrons from several species of nuclei- see text Image from X. Roca-Maza, Phys. Rev C. **78**, 044332 (2008). It can be found with this doi: 10.1103/PhysRevC.78.044332

The reason the diffraction pattern in figure 1.5 does not go to zero is that the nucleus is not exactly a hard sphere. If you go to the research paper referenced in figure 1.5, you will see charge density profiles derived from experimental scattering studies. For interest, you can take a look and see how well they compare to the simple model in figure 1.6.

We see from above that our definition of nuclear size has the radius, R_0 set to where the density is half of the peak density. There are other definitions of the nuclear size, that can depend on the method used and may depend on if it is mass density or charge density being measured. We will not go into detail in this course, but the constant at the front of expression 1.14 is usually quoted in a range of about 1.1-1.3.

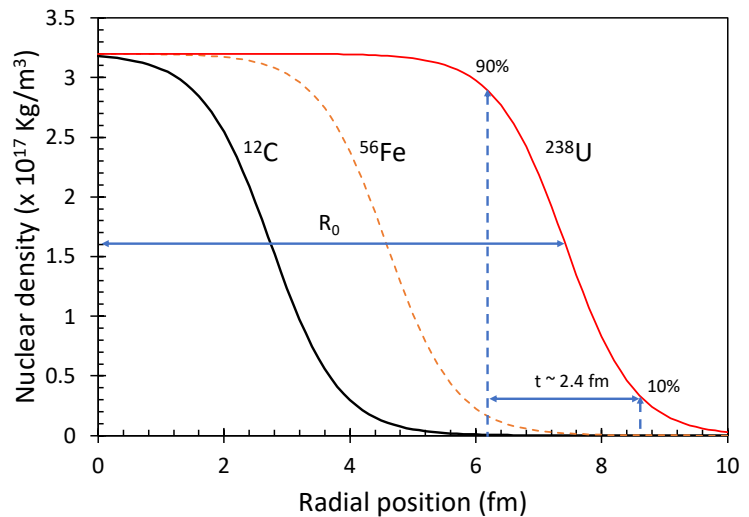


Figure 1.6 A schematic of the density profile for light and heavy nuclei. R_0 is defined where the density is half the maximum. The region, t , has a width that is independent of the atomic mass number, A .

CHAPTER 2: NOTES ON THE INTER-NUCLEON POTENTIAL

Requirements for the inter-nucleon force

- Needs to be strong to overcome the Coulomb repulsion of the protons. For example, use the result of Chapter 1 to calculate the radius of a Au nucleus and estimate the repulsive potential for a proton located at the edge of the nucleus. Or consider just that at 1 fm separation the Coulomb potential between two protons is about 1.4 MeV.
- We think it is short range for the following reasons;
 - a) The binding energy per nucleon, B/A is about constant. This means that, as we remove nucleons, the binding of the others remains much the same. This is in contrast to the long range Coulomb potential binding electrons to the shells of an atom- as we ionise it, the ionisation potential for further removal of electrons increases rapidly.
 - b) An explanation of this is that the nuclear forces are “saturated”. This means that a nucleon binds strongly only to those close to it $\sim 1-2$ fm away. This has the result that if a nucleon is removed from a large nucleus then the remaining nucleons are still surrounded by a similar number of other nucleons and so bound to the same degree.

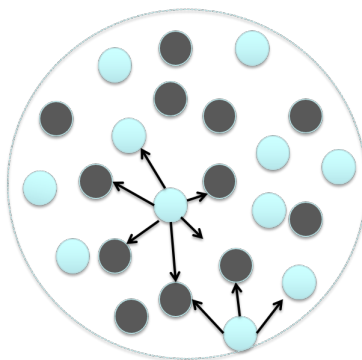


Figure 2.1 illustration of how removing one nucleon does not alter the binding of the remaining nucleons if there is only short range interaction. The nucleons remain bound by interactions to roughly the same number of “nearest neighbours”.

- c) Rutherford Scattering experiments show that the Coulomb interaction works very well until the closest approach of the scattering particles gets very small (of order 2 fm). This suggests a new force comes in to play at short range. See the assignments for a sample calculation.

- We know the density is roughly constant in the centre of the nucleus (from scattering experiments) and this implies that nucleons don't simply come closer and closer- there is a repulsive element to the potential at close range.
- We know the potential well formed must be at least ~8 MeV deep as that is the energy required to remove a nucleon (we see later that it is several times deeper than this).

In order to study the internucleon force theoretically, we can start by guessing roughly a shape. If we take the deuteron as an example we approximate it as a square well potential- see figure 2.2 below.

The deuteron

The deuteron is the simplest nucleus we can have that involves internucleon binding. Experimentally, we know the deuteron has no excited states and the binding energy is 2.224 MeV and the nuclear magnetic moment is $\mu \sim 0.86\mu_N$. We assume a square well depth V_0 and a radius, w and spherical symmetry (the ground state is 3S has no angular momentum in this case) and solve the Schrödinger equation;

$$\left(\frac{-\hbar^2}{2M_{red}} \nabla^2 + V_0 \right) \psi = E_0 \psi \quad (2.1)$$

where M_{red} is the reduced mass $M_{red} = M_p M_n / (M_p + M_n)$ and $E_0 = -B$, where B is the binding energy, which is a positive number here. As in atomic physics we have a solution;

$$\psi_{nlm} = R_{nl}(r) Y_{lm}(\phi, \theta) \quad (2.2)$$

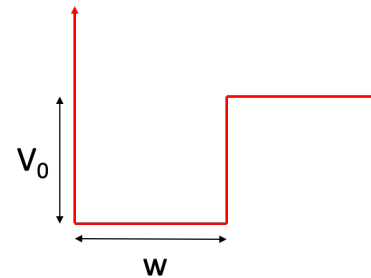


Figure 2.2 Approximate well used for initial solution of deuteron.

Where we separate the spherical harmonics Y and the radial function R . The quantum number n is not the same, however, as in atomic physics. It is the "radial" quantum number and is related to the 'principal' quantum number and angular momentum by

$$n_{radial} = n_{principal} - l \quad (2.3)$$

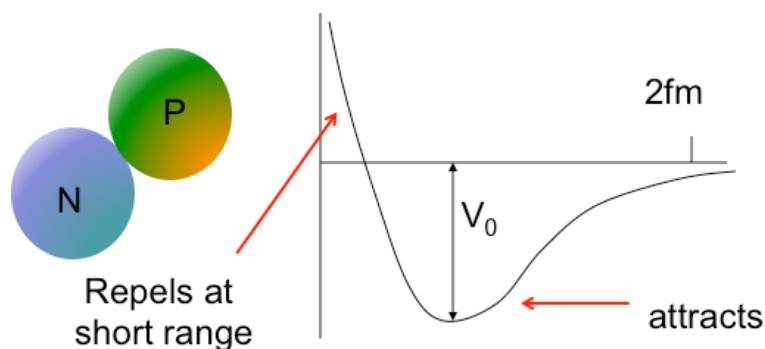


Fig. 2.3. Sketch of possible potential well for the inter-nucleon force. Not the steep rise as the potential becomes repulsive (positive potential) at short range and becomes zero far away.

In simple terms, it is the number of nodes in the radial eigenfunction. In some books (mostly older ones) it differs from this definition by 1 so that the smallest value is 0- we will use the above definition so that minimum value is 1. (This is a prime example of atomic and nuclear notation being different!) Now for the deuteron we have the ground state with $l = 0$. Both the neutron and proton have spin = $\frac{1}{2}$ and they are aligned for the deuteron so that $J = 1$ and thus we have 3S_1 as the ground state, where the notation is ${}^{2S+1}L_J$. The aligned spins imply that the magnetic moments should be aligned and we find this is indeed the case. For a proton we have $+2.79 \mu_N$ and for the neutron we have $-1.91 \mu_N$. Their total is $+0.88 \mu_N$ and this compares well to the actual value given above. A solution for the square well can be found using the standard approach (see Eisberg and Resnick Chapter 6). We re-write the Schrödinger equation, for $l = 0$, as:

$$\left(\frac{-\hbar^2}{2M_{red}} \nabla^2 + V(r) \right) U(r) = E_0 U(r) \quad (2.4)$$

where

$$R(r) = \frac{U(r)}{r} \quad (2.5)$$

and we have two regions, one inside the potential well and the other outside

- 1) $r < w$ and $V(r) = -V_0$
- 2) $r > w$ and $V(r) = 0$

The solutions are well known. For region 1)

$$U(r) = A \sin(k_1 r) + C \cos(k_1 r) \quad (2.6)$$

where

$$k_1 = \sqrt{\frac{2M_{red}(V_0 - E)}{\hbar^2}}$$

and $E = -B$ and $C = 0$. For region 2)

$$U(r) = D e^{-k_2 r} + F e^{k_2 r} \quad (2.7)$$

where

$$k_2 = \sqrt{\frac{2M_{red}B}{\hbar^2}}$$

and $E = -B$ and $F = 0$. We need to match solutions at $r = w$ and obtain;

$$A \sin(k_1 w) = D e^{-k_2 w} \quad (2.8)$$

We also require a smooth function so the gradients of $U(r)$ match at boundary;

$$A k_1 \cos(k_1 w) = -\beta D e^{-k_2 w} \quad (2.9)$$

Dividing these two equations leads to

$$\cot(k_1 w) = \frac{-k_2}{k_1} \quad (2.10)$$

Now, we do not know yet what w and V_0 should be but we can put in;

$$\cot(k_1 w) = \sqrt{\frac{B}{V_0 - B}} \quad (2.11)$$

With some numerical effort we can get results. We assume $B \ll V_0$ since we know, from experiment, that $B = 2.224$ MeV and have already noted that we think $V_0 > 8$ MeV due to the known binding of last nucleons in many nuclei and the consideration of the potential between protons. If we do this, we equate the RHS of the above equation to zero (assuming it is $\ll 1$) and have;

$$\cot(k_1 w) = 0$$

which leads to solutions of $k_1 w = \pi/2, m\pi/2$ etc, where m is an integer. Taking the first solution, we get;

$$k_1 w \sim w \sqrt{\frac{2M_{red}V_0}{\hbar^2}} \sim \frac{\pi}{2} \quad (2.12)$$

which leads further to;

$$V_0 \sim \frac{\pi^2}{4w^2} \frac{\hbar^2}{2M_{red}} \quad (2.13)$$

This gives us

$$w^2 V_0 \sim \frac{\pi^2}{4} \frac{\hbar^2}{2M_{red}} \sim 10^{-28} \text{ MeV m}^2 \quad (2.14)$$

If we approximate $w \sim 2$ fm, based on observations of Rutherford Scattering, then we have $V_0 \sim 25$ MeV justifying the earlier assumption that $B \ll V_0$. A more sophisticated calculation gets V_0 closer to ~ 37 MeV. If we join up the solutions for $U(r)$ inside and outside the potential well, we have something like Figure 2.4 below. There is some chance of the nucleons being located out of the potential well region. This is typical quantum well behaviour.

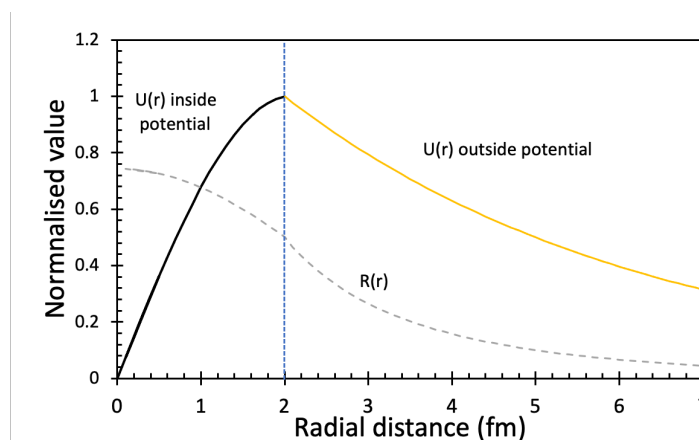


Fig 2.4 Sketch of normalised wave-function solution for well depth and shape assumed. Note how $R(r)$, the radial wavefunction, extends well beyond the potential well region marked by the vertical line at $r=2$ fm.

Additional observations on Deuterium.

- Experimentally only the $J = 1$ nuclear spin state is bound with 2.224 MeV binding.
- This implies that the potential must be spin dependent to have the $J = 0$ solution unbound.
- Scattering data for proton-neutron interactions suggests the following

$$\begin{array}{ll} J=1 & V_0 = 31 \text{ MeV and } w = 2.2 \text{ fm} \\ J=0 & V_0 = 13.4 \text{ MeV and } w = 2.65 \text{ fm} \end{array}$$

For a quantum well, the lowest state is not given by V_0 but, for the case of a deep well the states vary as

$$E \sim \frac{n^2}{w^2} \quad (2.15)$$

The narrowness of the potential well means that for the $J=1$ case, the first level is only just below the top of the potential well and the lower depth for the $J=0$ case means there is no bound state within the potential. Clearly the spin orientations make a difference and we can consider this with other observations now. The inter-nucleon potential is written now as;

$$V = V_c + V_s = f_c(r) + f_s(r)\mathbf{s}_1 \cdot \mathbf{s}_2 \quad (2.16)$$

Where V_c is the normal central component dependent on the separation of the nucleons and the second term is dependent on the individual spins, \mathbf{s}_i . We see that with the dot product the orientation either makes the potential deeper or shallower.

Quadrupole moment of the deuteron

We also observe that the quadrupole for the deuteron moment is non-zero experimentally. However, if we have a zero angular momentum state as we have stated, then that implies spherical symmetry in the wavefunction and a zero quadrupole moment. The reason for this apparent discrepancy is that we in fact have a mixture of states for the ground state of deuterium. Some possible additions to the 3S_1 are

$${}^1P_1 \quad {}^3P_1 \text{ or } {}^3D_1$$

The first two are discounted as they have opposite parity to the 3S_1 and parity, being related to angular momentum, should be a conserved property, we therefore have a small component of 3D_1 mixed in. The total wave-function is then

$$\psi_{tot} = (1 - \varepsilon)^{1/2} \psi({}^3S_1) + \varepsilon^{1/2} \psi({}^3D_1) \quad (2.17)$$

where $\varepsilon \sim 0.05-0.08$. This happens because there is a tensor component to the inter-nucleon potential that favours it. This means, in practice, that the interaction between the nucleons depends not only on their orientation but their separation spatially relative to the spin.

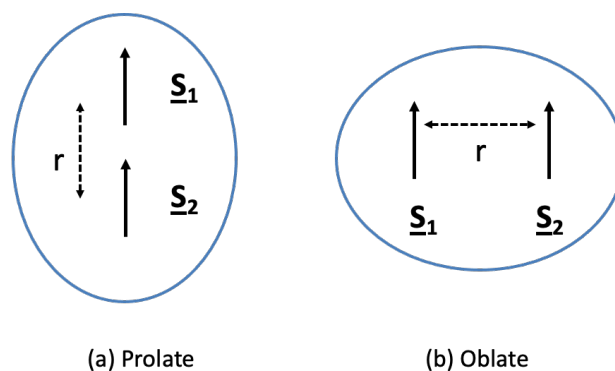


Fig 2.5. Schematic of two ways for the spins to align and interact in deuterium

Figure 2.5 shows the spins aligned in two ways, both give a distorted nucleus. Experimentally the quadrupole moment for deuterium is $Q > 0$ so the prolate shape is favoured. The tensor part of the inter-nucleon potential is written;

$$V_T = f_T(r) \left[\frac{3(\mathbf{s}_1 \cdot \mathbf{r})(\mathbf{s}_2 \cdot \mathbf{r})}{r^2} - (\mathbf{s}_1 \cdot \mathbf{s}_2) \right] \quad (2.18)$$

which has a value dependent on the orientation of the spins of the two nucleons as well as the direction in which they are separated.

The spin-orbit potential

Extensive scatter experiments at high energy ($\text{GeV} = 10^9 \text{ eV}$) with protons and neutrons shows the existence of a spin-orbit part of the potential. This is written;

$$V_{LS} = f_{LS}(r) \mathbf{L} \cdot (\mathbf{s}_1 + \mathbf{s}_2) \quad (2.19)$$

where \mathbf{L} is the relative angular momentum of the nucleons. This is a nuclear analogue of the spin orbit interaction that you will have come across in atomic physics.

Charge independence

We note the existence of “mirror nuclei” which have the same odd number of nucleons but swap a proton for a neutron. For example $^{17}\text{O}^8$ and $^{17}\text{F}^9$ where we have respectively $Z=8, N=9$ and $Z=9, N=8$. The first few energy levels are tabulated in figure 2.6, as we see, there is a great similarity. This and other examples shows the charge independence of the inter-nucleon force— as far as it is concerned neutrons and protons are basically the same particle. In summary, the inter-nucleon potential is much more complicated than the Coulomb potential and has several components. This is due to the more complex structure of the nucleons. They are in fact made up of other particles, quarks.

| ¹⁷ O ⁸ | ¹⁷ F ⁹ |
|------------------------------|------------------------------|
| 5.08 | 5.1 |
| 4.55 | 4.69 |
| 3.85 | 3.86 |
| 3.06 | 3.10 |
| 0.87 | 0.50 |
| 0.0 | 0.0 |

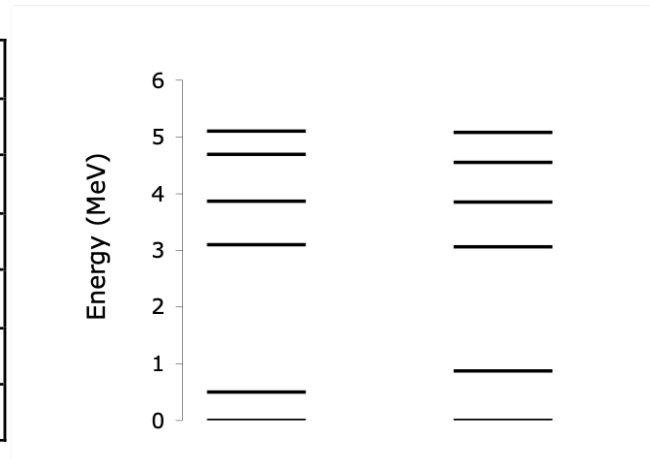


Figure 2.6 Similarity in energy levels for mirror nuclei illustrates how the internucleon interaction is essentially same for protons and neutrons.

Meson Exchange

For the Coulomb interaction present day QED theory (which is accurate to 11 decimal places!) states that a virtual photon is exchanged when particles interact, as shown in figure 2.7. The photons exist only in the interaction and energy and momentum must be conserved overall. They are massless and the range is effectively infinite. In 1935 Yukawa suggested that the short range of the nuclear force was due to the fact that it is mediated not by photons but by exchange of heavy particles.

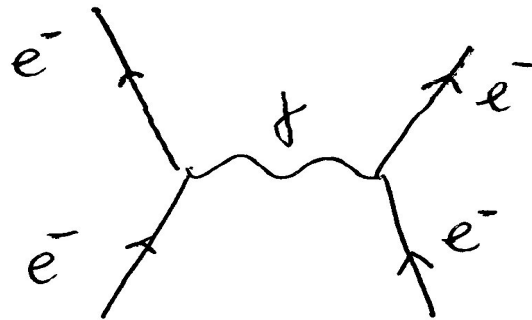


Fig 2.7. Feynman diagram for interaction of electrons by exchange of a photon.

Recall the uncertainty relation; $\Delta t \Delta E \sim \hbar/2$, we can “borrow” energy ΔE for a time Δt . If we create a particle with mass M we need to do this in a time;

$$\Delta t \sim \frac{\hbar}{2Mc^2} \quad (2.20)$$

If we assume the interaction happens at the speed of light then the range $R \sim c\Delta t$ and we have

$$R \sim \frac{\hbar}{2Mc} \quad (2.21)$$

Now, we require $R \sim 1$ fm to match the typical distance between nucleons in a nucleus and thus we require $M \sim 200m_e$. This is an intermediate mass between the electron and the nucleon and so such particles were dubbed “mesons” and it was postulated that these may also play a role in the exchange of protons for neutrons and vice versa. Yukawa proposed a potential of the form;

$$V(r) = \frac{g_s^2}{4\pi} \frac{e^{-r/R}}{r} \quad (2.22)$$

where g_s acts like the electrons charge in e-m interactions. We can roughly estimate g_s by considering $V \sim 30\text{MeV}$ at $r = 2\text{fm}$. We get;

$$\frac{g_s^2}{4\pi} = 10^{-26} \text{ Jm} \quad (2.23)$$

and we further get to;

$$\alpha_s = \frac{g_s^2}{4\pi\hbar c} \sim 1 \quad (2.24)$$

which we can compare to the atomic physics fine structure factor which $\sim 1/137$. This means relative to the electromagnetic interaction the so called strong nuclear force is ~ 100 times stronger.

Pions

In fact mesons have been found in particle physics experiments in 1947. They are also found at high altitude where cosmic rays with high energy interact in the atmosphere. The so called π mesons (pions) have been found with 3 types with different electronic charges;

$$\pi^+ \quad \pi^- \quad \pi^0$$

The masses are;

$$\begin{aligned} M_{\pi^+} &= M_{\pi^-} = 273.1m_e \\ M_{\pi^0} &= 264.1m_e \end{aligned}$$

They have odd parity and spin 0. They are unstable and the π^+ , π^- decay in $\sim 10^{-8}\text{s}$ to a muon and a neutrino. The π^0 decays in $\sim 10^{-16}\text{s}$ to two photons (gamma rays). The strong force is mediated by the exchange of these mesons. Figure 2.8 shows possible interactions where exchange of a pion can change the identity of a nucleon. Interaction with a neutral pion just leads to scattering, but with the charged pions the protons can become neutrons and vice-versa.

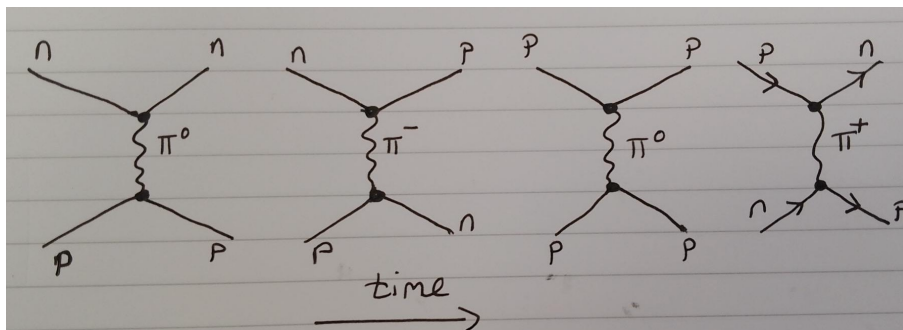


Fig 2.8. Feynman diagrams for the exchange of mesons as a means of nucleon interaction.

A detailed study (beyond L2) shows that the predicted potential with these particles matches the observations we have made. The potential in particular

- Has short range
- Is dependent on spin
- Has a tensor part
- Is charge independent
-

However, pion exchange does not work so well for very short range $< 1\text{fm}$. Closer in we consider heavier mesons, that have since been discovered

| | | |
|----------|----------------------|----------------|
| ρ | $770 \text{ Me}/c^2$ | $\sim 1500m_e$ |
| ω | $783 \text{ Me}/c^2$ | $\sim 1530m_e$ |

These rho and omega mesons result in a repulsive potential between nucleons when the range is about 0.5 fm . This prevents nucleons from getting very close and explains why the density of nuclear material is about constant for all nuclei.

CHAPTER 3: MODELS OF THE NUCLEUS

3.1 Liquid drop model

This is a model, developed first by George Gamow, based on classical physics considerations. The nucleus acts as a collective liquid (see collective model below). Apart from the mass of the constituent nucleons, the mass is considered to be due to several contributions, each of which reduces or increases binding energy. *In the following we express masses in their mass-energy energy units (MeV)- it saves us writing c^2 every time.* The contributions are

1. The mass-energy of constituents of the nucleus;

$$M_{\text{Nuc}} c^2 = ZM_p c^2 + (A-Z)M_n c^2$$

where we would usually put the mass energy in MeV units.

2. Volume binding energy, in MeV due to binding of A nucleons;

$$M_v c^2 = -a_v A$$

3. Surface tension energy: **As in a liquid drop**, the outer nucleons are not bound so tight as they do not experience binding from all sides. This reduces binding and the energy term is proportional to surface area which scales as R^2 and thus $A^{2/3}$;

$$M_s c^2 = a_s A^{2/3}$$

We can see in figure 3.1 how surface nucleons have fewer close neighbours to interact with.

4. Coulomb energy term. There are Z protons and they have a repulsive electrostatic potential energy;

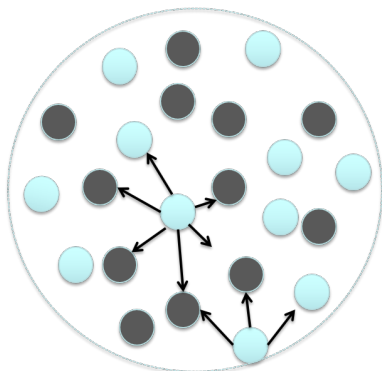


Figure 3.1 We can see that a surface nucleon will likely have fewer nearest neighbours to bind to than a nucleon in the centre.

$$\frac{3}{5} \frac{(Ze)^2}{4\pi\epsilon_0 R}$$

where R is the nuclear radius which is proportional to $A^{1/3}$. Thus, we have a reduction in binding,

$$M_{cc} c^2 = a_c Z^2 / A^{1/3}$$

5. The asymmetry term. We have noted in section 1 the preference to have $N > Z$ at high A values but $N \sim Z$ at low A values. Later, we will explain, in terms of the Pauli exclusion, $N > Z$ reduced binding but having $N = Z$ causes more Coulomb repulsion. For now, the term that reduces binding due to this asymmetry is

$$M_{AS} c^2 = a_{AS} \frac{(A - 2Z)^2}{A}$$

6. The odd-even term: We have seen that there are far more even-even nuclei and that odd-odd is least likely. This term is given in different forms by different authors, one version has;

$$\begin{aligned} \delta(A,Z) &= -a_{OE} && \text{even-even} \\ \delta(A,Z) &= 0 && \text{odd-even or even-odd} \\ \delta(A,Z) &= +a_{OE} && \text{odd-odd} \end{aligned}$$

Where we also normalise to the atomic mass number with a scaling of $A^{3/4}$ as seen below. This is a purely empirical scaling that is chosen to fit the data. Gathering these terms together we get an equation for the mass of nuclei (remember it is in energy (MeV) units here).

$$M(A,Z)c^2 = ZM_p c^2 + (A - Z)M_n c^2 - a_V A + a_S A^{2/3} + \frac{a_C Z^2}{A^{1/3}} + a_{AS} \frac{(A-2Z)^2}{A} + \frac{\delta(A,Z)}{A^{3/4}} \quad (3.1)$$

Least squares fit to real data on the masses indicate that good values for the parameters, (due to AES Green) in units of MeV are;

$$\begin{aligned} a_v &= 15.76 \\ a_s &= 17.81 \\ a_c &= 0.711 \\ a_{as} &= 23.702 \\ a_{oe} &= 34.0 \end{aligned}$$

Dropping the c^2 for simplicity, the binding energy is then;

$$B = [ZM_p + (A - Z)M_n - M(A,Z)] \quad (3.2)$$

which can be expressed as

$$B(\text{MeV}) = a_V A - a_S A^{2/3} - \frac{a_C Z^2}{A^{1/3}} - a_{AS} \frac{(A-2Z)^2}{A} - \frac{\delta(A,Z)}{A^{3/4}} \quad (3.3)$$

And the binding energy per nucleon is;

$$B/A = a_V - \frac{a_S}{A^{1/3}} - \frac{a_C Z^2}{A^{4/3}} - a_{AS} \frac{(A-2Z)^2}{A^2} - \frac{\delta(A,Z)}{A^{7/4}} \quad (3.4)$$

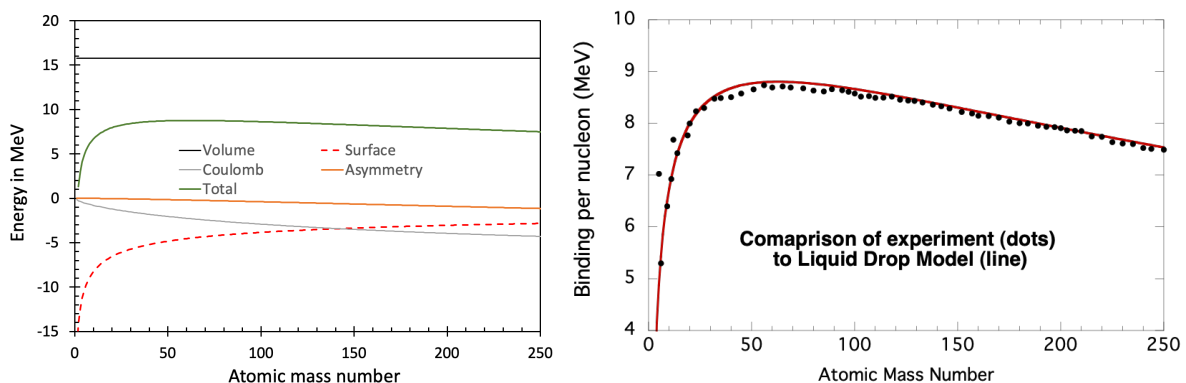


Figure 3.2 Left: Binding energy per nucleon from the liquid drop model, showing some individual contributions. Note how the Coulomb term grows in magnitude with A but the surface term drops. Right: Comparison of liquid drop model with data.

Figure 3.2 shows a plot of the results ignoring the asymmetry and odd-even terms and assuming $Z=0.4A$. We can see that it matches the experimental data we saw previously.

A success for the liquid drop model

In the next chapter, we shall discuss alpha decay, which is a process by which a heavy element emits a helium nucleus, which is called an alpha particle. If we compare the binding energy of the initial (parent) nucleus with the binding of the daughter nucleus and the alpha particle, we can get define the Q value of the reaction, which is the energy released

$$Q = E_B^{final} - E_B^{initial} \quad (3.4)$$

and plot as in figure 3.3. We can see that Q is positive, only for atomic masses of about 150 and more. What this means is that alpha decay is only expected to be an exothermic reaction for large atomic masses and we don't expect to see it for lower mass elements. Experimental evidence tells us that there are in fact no emitters with atomic mass lower than 140. This is in pretty good agreement with what the liquid drop model predicts.

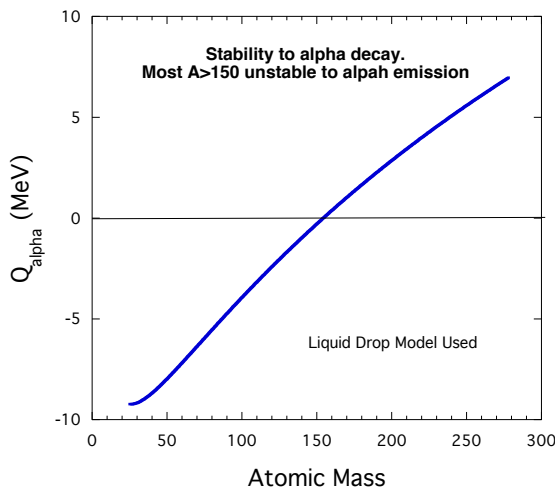


Figure 3.3 Expected Q value for alpha decay calculated with the liquid drop model.

Limitations of the liquid drop model

If we look in detail and the binding energy curve, we see that there is not a smooth line but oscillations in binding per nucleon. We see in figure 3.4, for example, that ^4He and ^{12}C have binding above the trend line- that is to say they are particularly stable. In addition to this, the model gives no information on important properties such as the dipole and quadrupole moments. Before addressing these with more sophisticated models, we first discuss another thing that is not addressed by the liquid drop model- magic numbers which we explore next.

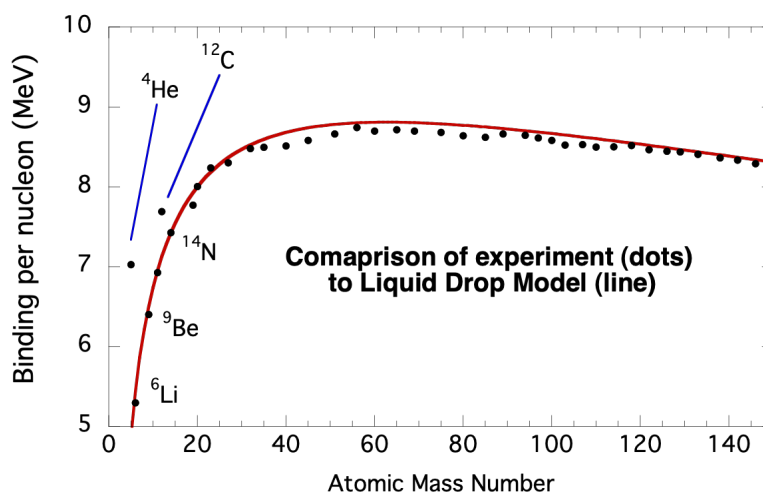


Figure 3.4 Detail of liquid drop model vs experiment

Magic Numbers

The formula in the liquid drop model is good for the overall trend of binding energies. However, it does not get the fine detail of variation in binding energy. One thing in particular it fails to explain is so called *Magic Numbers*. It is seen that for example that;

- For $Z=20, 28, 50$ and 82 there are a higher number of stable isotopes than for nearby elements (see figure 3.5).
- There are more stable isotones (N same) for $N=20, 28, 50, 82$ and 126 than for nearby N values.

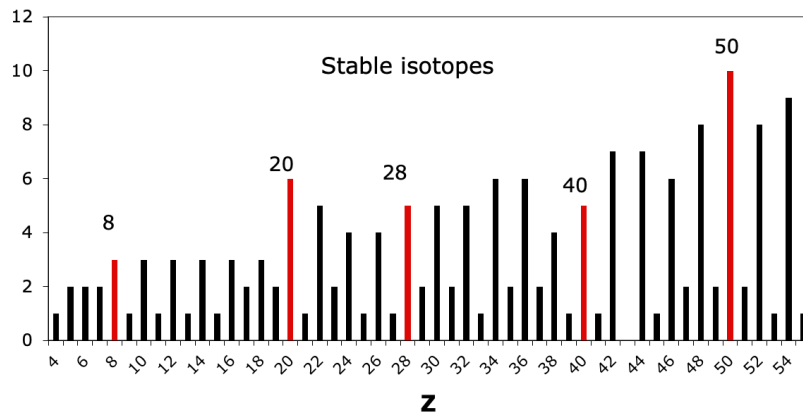


Figure 3.5 Number of isotopes for elements as a function of Z . Note also the oscillation from odd to even numbers

- There are peaks in the binding energy of the last nucleon compared to liquid drop model predictions for both neutrons and protons associated with these “magic” numbers.
- There are also severe falls in neutron capture rates (figure 3.6) when the number of neutrons is a magic number- this indicates that the nucleus is already particularly stable and adding another neutron is not energetically favourable.

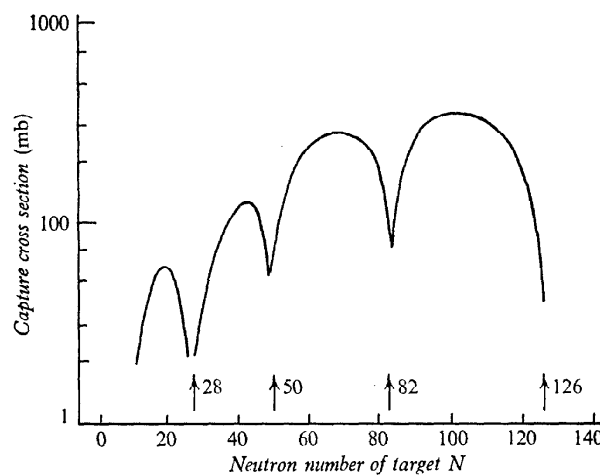


Figure 3.6 Capture rate for neutrons as a function of N . Note how the rate falls close to magic numbers. Other data regarding Magic numbers will be presented in the lectures.

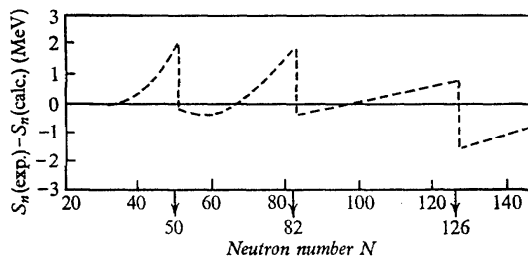


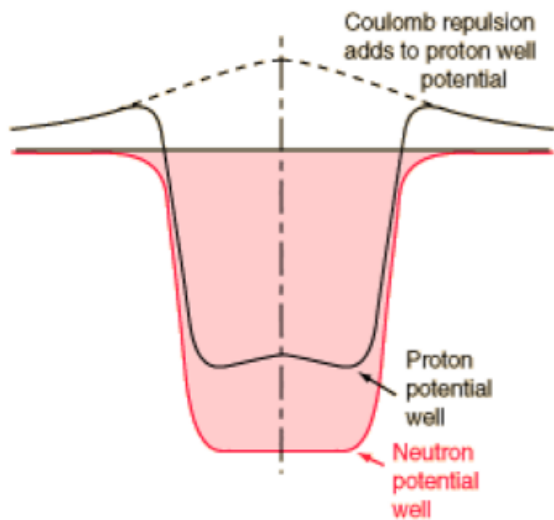
Figure 3.7 Neutron removal compared to a liquid drop calculation. Peaks at 50,82 and 126 are seen.

Other evidence for magic numbers is that the removal energy for a neutron or proton shows peaks relative the liquid drop model at particular numbers. We can see, for example, in figure 3.7 that there appears to be extra stability, that is to say, higher binding energy at some particular values of neutron number. Similar data is seen for protons and at the same numbers. In the next section, we

discuss the shell model and how this can help explain the magic numbers.

3.2 The shell model

This is the basis of our understanding of the magic numbers. It assumes that the nucleons move about independently in a roughly constant potential well that is due to the net interaction of all the other nucleons. We can perhaps compare to the Hartree model in atomic physics. This model generally results in a potential of the form seen below- the so called Wood-Saxon form is often used as in the equation accompanying figure 3.8



$$V(r) = \frac{-V_0}{1 + \exp\left(\frac{r-R}{a}\right)}$$

Figure 3.8 Schematic of potential for nucleons. Note how the proton potential has a Coulomb 'Hill' due to repulsion of incoming protons by the nucleus.

where we can see that there is difference at the boundary for protons due to the Coulomb repulsion. We normally think of this as a spherically symmetric potential for which we solve the Schrödinger equation. In this was we develop orbitals with quantum numbers n and l where n is the radial quantum number. Our previous discussion indicates that for a large nucleus:

$$V_0 \sim 30-50 \text{ MeV} \quad \text{and} \quad R \sim 1.2A^{1/3}$$

It turns out that the exact shape does not affect our basic conclusions. We can numerically solve the Schrödinger equation and we get energy eigenvalues that depend on both n and l . The radial quantum number is related to the principle quantum number by:

$$n_p - l = n_{\text{radial}} \quad (3.5)$$

In nuclear physics we use $n = n_{\text{radial}}$ so we can have the 1s,1p,1d etc . (Some books have a slightly different definition and have 0s, 0p etc as the lower levels). With the addition of a spin-orbit interaction

$$V_{\text{SO}} = f(r)\mathbf{L} \cdot \mathbf{S} \quad (3.6)$$

we get the energy levels in figure 3.9 below, where similar to the atomic case,

$$f(r) = \frac{1}{r} \frac{dV}{dr} \quad (3.7)$$

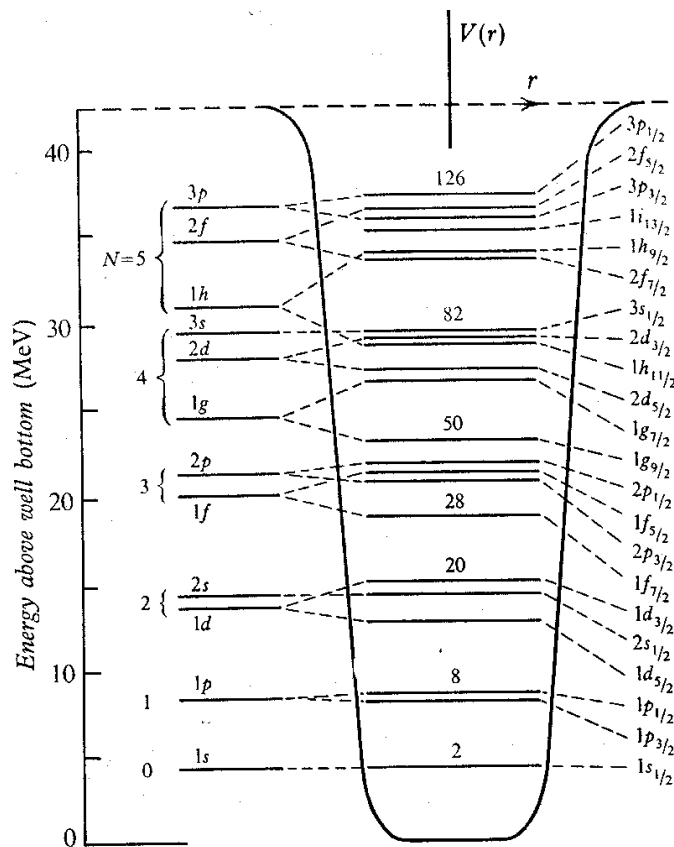


Figure 3.9 Schematic of the shell model with (right) and without (left) the spin-orbit interaction. Notice the large energy gaps that appear at the 'magic' numbers. Neutrons and protons both separately fill such a shell structure.

We can note that the splitting gives higher energy for the lower J case where $j=l\pm 1/2$ for the nucleons which have spin = 1/2. Some of the important results of the shell model are;

1. We get magic numbers corresponding to filled sub-shells and there is a large gap to the next energy level. This explains the stability of nuclei with magic number of either protons or neutrons or in some cases both.

- The closed shells have net $J = 0$ as the m_l values are paired off in shells. Even-even nuclei always experimentally have $J=0$.
- The parity should be $P = (-1)^l$ so a closed sub-shell should have parity = +1. Such nuclei should have notation $J^P = 0^+$
- Additional nucleon outside a closed shell should contribute the nuclear spin and parity. For example ^{17}O has an additional neutron in the $1d_{5/2}$ level. Thus we predict for the nucleus

$$J = 5/2, \quad l = 2 \text{ and } P = (-1)^2 = +1$$

$$J^P = 5/2^+ \text{ agrees with experiment}$$

- There is a similar story for nuclei missing a nucleon from a closed sub-shell. For example $^{15}\text{N}^7$ has missing proton in $1p_{1/2}$ sub-shell. We expect the nucleus to thus have a parity of $(-1)^l = -1$ (since $l=1$) and a spin of $1/2$. Experimentally this is so.
- Many other cases are predicted correctly- but not all- there is still some nucleon-nucleon interactions that is not accounted for in the independent nucleon model we have used.

An exception

An exception is ^{107}Ag , with $Z=47$, $N=60$. It should have 7 protons in the $1g_{9/2}$ level and thus the J^P should be $9/2^+$ since $l=4$ and the other nucleons pair off. In fact, experimentally, we have $J^P=1/2^-$ because it is energetically more favourable to have 8 protons in the $1g_{9/2}$ level and a missing proton in the $2p_{1/2}$ level below. This is an effect of the nucleon-nucleon pairing force which is strongly dependent on l and the $1g_{9/2}$ level has high value. There are other exceptions but the overall the shell model gets the spin and parity right in many cases.

Odd-even effect

Consider that the inter-nucleon interaction is attractive so that the lowest energy should be when they are close together. However, Pauli exclusion keeps them apart if the quantum numbers are the same. Thus the best pairing should be between nucleons with j, m_j and $j, -m_j$ for a given sub-shell as the orbits are similar but we have one quantum number different. This means that the angular momentum is paired off to be zero overall. For even-even nuclei we have every nucleon paired off and so the average binding per nucleon can be higher and they are more likely to be stable than an odd-even or even-odd nucleus. This observed odd-even effect was accounted for, we recall, in the liquid drop model. It turns out that all even-even nuclei are $J^P = 0^+$.

N and Z similar at low A

The fact that the neutrons and protons both fill a shell structure helps us to understand why at low Z it is beneficial to have similar numbers. Look at the figure below (figure 3.11). For a

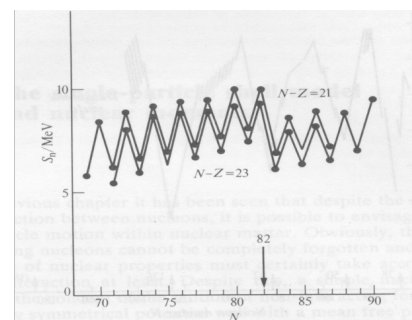


Figure 3.10 Binding of 'last' neutron in isotopes keeping $N-Z$ constant at 21 and 23. Note the odd-even effect and change at the magic number 82.

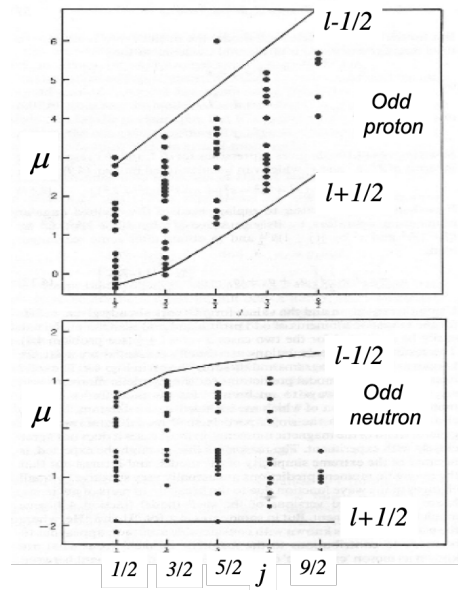


Figure 3.12 Schmidt plot of the measured magnetic moments against the predictions of the Shell model. The prediction shows two lines in each case since we can have $j = l+1/2$ or $l-1/2$.

Electric quadrupole moments

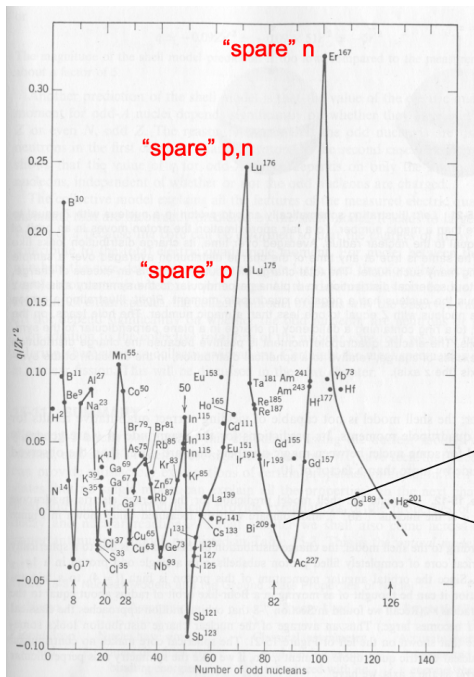
We have noted in Chapter 1, that the electric quadrupole moment for a distribution of charge can be written;

$$Q_0 = \int \rho(\mathbf{r})(3z^2 - r^2) dV \quad (3.11)$$

This will be positive or negative according to the shape. For an ellipsoid stretched along the z -axis it will be positive since maximum z will be higher than the other 2 dimensions and so $3z^2 > r^2$. In a QM treatment we get a slightly more subtle answer in that;

$$Q = Q_0 \frac{2J-1}{2(J+1)} \quad (3.12)$$

for $J > 0$ only. This means we expect $Q=0$ for $J=1/2$ as well as $J=0$. Since $J=0$ for a closed shell, we expect then that the quadrupole moment would be given by the outer nucleon for odd A elements where there is a 'spare' proton. For a spare neutron we don't expect a quadrupole moment since it carries no charge. In figure 3.13 we present some data on measured electric quadrupole moments. In fact, what is seen experimentally is that there is little difference between having an outer proton or neutron and that for some ranges there is exceptionally high values. The understanding of these facts centres about the fact that nucleons interact strongly and an unpaired nucleon can drag other nucleons out of a spherical configuration. In this way nuclei with only an unpaired neutron can have a high quadrupole moment.



| Isotope | Q / m^2 |
|------------------|-------------------------|
| ³⁵ Cl | -8.0×10^{-30} |
| ³⁷ Cl | -6.32×10^{-30} |
| ³³ S | -5.0×10^{-30} |

No obvious connection to whether spare proton or neutron

Note close to zero near closed shells

e.g. ²⁰⁹Bi has 126n and 83p

e.g. ²⁰¹Hg has 121n and 80p

Figure 3.13 Data on electric quadrupole moments for various elements arranged by the number of nucleons for the type that has an odd number. Note the fall in Q as we are close to a magic number and how having a "spare" n or p makes little difference.

3.3 Collective effects

- The shell model has nucleons moving independently in a net potential.
- The collective model harks back to the liquid drop model.
- Individual nucleons can have asymmetric orbits depending on the angular momentum
- For nuclei away from closed shells the nucleus can be highly distorted with significant quadrupole moments
- In the 1950s the collective model was developed

Consider an even-even nucleus with close to filled sub-shells. We expect from the shell model to have a nearly symmetrical spherical nucleus. The odd nucleon or "hole" moves independently in the net potential. We need to consider the possibility that the orbit of this lone nucleon or "hole" can be highly asymmetrical, depending on the value of l and can in turn cause distortion of the nuclear shape leading to significant quadrupole moments.

There is the possibility of excited states for these nuclei corresponding to oscillations in the shape. These are collective motions of the nucleons and hence the name "collective model". This can lead to deformation as in figure 3.14.

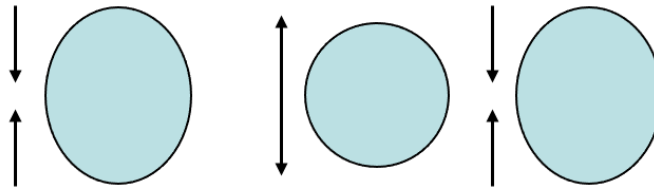


Figure 3.14 The most basic nuclear oscillation

We have a quantum system here and the energy of the oscillations is $E = \hbar\omega$ and the oscillations lead to a description of the nuclear surface as

$$r = r_{av} + \sum_{l=1}^{l=\infty} \sum_{m=-l}^l a_{lm} Y_{lm}(\theta, \phi) \tag{3.13}$$

where the $Y_{lm}(\theta, \phi)$ are spherical harmonics with l the angular momentum quantum number and m , the z-component where a_{lm} is an amplitude. The $l = 1$ case leads to a shift of the centre of the nucleus that cannot come from internal forces and so the most basic, ellipsoidal deformation is associated with $l = 2$ and

$$r = A + BY_{20}(\theta) \tag{3.14}$$

for the radius, where Y_{20} is the spherical harmonic corresponding to $l=2$.

$$Y_{20}(\theta, \phi) = \frac{1}{4} \sqrt{\frac{5}{\pi}} (3\cos^2\theta - 1) \tag{3.15}$$

which we can see, will represent an ellipsoidal shape. These collective vibrations are known as ‘phonons’ (compare to solid state physics). With 1, 2...etc phonons we get energy levels spaced by $\hbar\omega$ but with $l=2$ for each we are restricted to angular momentum of 0, 2, 4 etc An example of a vibrational nucleus is ^{114}Cd with quadrupole energy levels as below;

| | | | |
|---|----------------|---|-------------------------------------|
| $0^+, 2^+, 4^+$ <hr style="width: 100%;"/> | $2\hbar\omega$ | 4^+ <hr style="width: 100%;"/> 2^+ <hr style="width: 100%;"/> 0^+ <hr style="width: 100%;"/> | 1.283 MeV 1.208 MeV 1.133 MeV |
| 2^+ <hr style="width: 100%;"/> | $\hbar\omega$ | 2^+ <hr style="width: 100%;"/> | 0.558 MeV |
| 0^+ <hr style="width: 100%;"/> | 0 | 0^+ <hr style="width: 100%;"/> | 0 |

Figure 3.15 Vibrational energy levels of ^{114}Cd (right) compared with predictions of the collective model (left). Apart from the slight lifting of degeneracy for the $2\hbar\omega$ level, the fit is good.

We note that the theoretical degeneracy of the upper 0^+ , 2^+ and 4^+ levels is slightly lifted in experiment, but they are quite close. This is not the only sort of energy level. Far from magic numbers the distortion of the nucleus can be permanent and this means that we have the possibility of rotational energy levels (think about a comparison with molecules and atoms- the molecules are not spherically symmetric and we get rotational states which do not arise in monatomic gases, you will have come across this briefly in level 1). The energy levels are given by;

$$E_i = \frac{(Ang.Mom)^2}{2 \times Inertia} = \frac{J(J+1)\hbar^2}{2MI} \quad (3.16)$$

where MI is the moment of inertia. The spacing of the energy levels seen will give the value of the moment of inertia for the nucleus. Again, the ellipsoidal geometry restricts $J= 0,2,4 \dots$ etc for even-even nuclei. For ^{238}U some of the low lying states are seen below.

| 8^+ ————— 6^+ ————— 4^+ ————— 2^+ ————— 0^+ ————— | 0.523MeV 0.309MeV 0.148MeV 0.0447MeV 0 MeV | For ^{238}U the levels match expected ratio: <table border="0" style="margin-left: 20px;"> <thead> <tr> <th>Ratio</th> <th>Theory</th> <th>Expt</th> </tr> </thead> <tbody> <tr> <td>4+/2+</td> <td>3.33</td> <td>3.31</td> </tr> <tr> <td>6+/4+</td> <td>2.1</td> <td>2.09</td> </tr> <tr> <td>8+/6+</td> <td>1.71</td> <td>1.69</td> </tr> </tbody> </table> | Ratio | Theory | Expt | 4+/2+ | 3.33 | 3.31 | 6+/4+ | 2.1 | 2.09 | 8+/6+ | 1.71 | 1.69 |
|---|--|--|-------|--------|------|-------|------|------|-------|-----|------|-------|------|------|
| Ratio | Theory | Expt | | | | | | | | | | | | |
| 4+/2+ | 3.33 | 3.31 | | | | | | | | | | | | |
| 6+/4+ | 2.1 | 2.09 | | | | | | | | | | | | |
| 8+/6+ | 1.71 | 1.69 | | | | | | | | | | | | |

Figure 3.16 Low lying rotational states for ^{238}U . These states appear due to distortion of the nucleus.

The value of moments of inertia that arise from such spectra are generally a factor 2-3 lower than the expected value for a rigid body- suggesting that it is more fluid like. One interesting plot is a so called 'yrast' plot that plots angular momentum against frequency of rotation. The

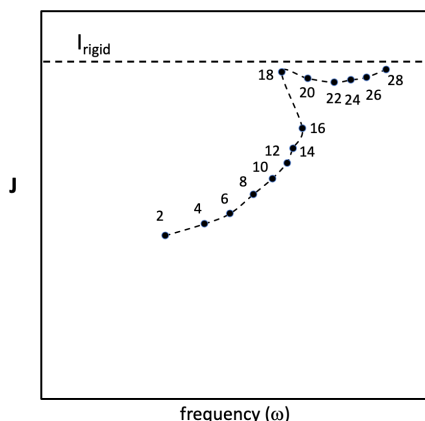


Figure 3.17 'yrast' plot for Dysprosium

angular momentum for Dysprosium increases as the nucleus rotates faster. For a rigid nucleus there should be a linear relationship. However, at some point the curve bends upwards and this is a result of additional distortion of the nucleus that increases the moment of inertia

What we see, (figure 3.17) is that for higher and higher values of J the rotation frequency increases as we would expect- at some point the frequency decreases. This is because there is distortion of the nucleus- this increases the moment of inertia and thus for a given rotational energy, the rotation frequency decreases. After this, the distortion is limited as nuclear forces

pull the nucleons back together.

3.4 Single particle energy levels in a non-spherical potential

So, far in our discussion of collective effects, we have considered energy levels due to dynamic effects of rotation and vibration. This, rather like in a molecule, leads to particular energy levels. However, some nuclei (typically $150 < A < 190$ and $A > 230$) have a permanent distortion from a spherical shape and this affects the single particle states that we have seen in our standard shell model shown above. In these cases, the orbital angular momentum, l is not a good quantum number. The orientation of the orbit relative to an axis of symmetry is important:

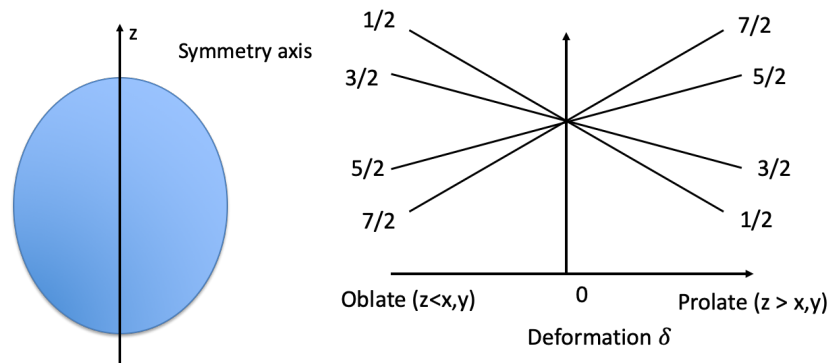


Figure 3.18 (a) Deformed nucleus as a rotational ellipsoid (b) energy level splitting in a deformed potential for $f_{7/2}$ state. The numbers give the projection of j onto the axis of symmetry.

The energy levels depend on the component of j that lies along the axis of symmetry. For example if we take the $f_{7/2}$ orbit (as in Krane), there is a degeneracy of 8, due to j_z running from $-7/2$ to $+7/2$. In a spherical potential they are degenerate but this degeneracy is lifted in a deformed potential. Symmetry means the positive and negative components are the same, so the level splits into 4. The ordering of the levels depends on the deformation being either oblate or prolate and the separation depends on the degree of deformation.

the half-life of ^{237}Np is only 2.14 million years and the chain decayed a long time ago. The other starting elements have half-lives of billions of years.

We can note that the appearance of β^- -decay in the chain. The reason for this is connected to our earlier observation of stability for nuclei depending on an increasing ratio of neutrons to protons as we move to heavier elements. As we undergo successive α -decays, we would change the number of protons and neutrons by an equal amount. However, in order to stay stable the daughter nuclei ought to lose neutrons at a slightly higher rate to move towards a ratio closer to 1:1 that is stable at lower masses. This is achieved by the β^- -decay that changes a neutron into proton at different points in the chain, moving the chain of decay products back to the line of stability.

Theory of alpha-decay

Gamow investigated the theory of α -decay some time ago and we will give a simple discussion of what can be a complex area of physics, when the details are looked into. The nucleus decays into a daughter nucleus and an α -particle. We can consider that the α -particle has two potentials acting on it. One of these is the nuclear binding potential that is short range and rather flat bottomed as seen in Chapter 3. The other is the Coulomb interaction between the α -particle and the daughter nucleus:

$$V = \frac{2Z_d e^2}{4\pi\epsilon_0 r} \quad (4.1)$$

We can understand how we can create a potential well from the nuclear and Coulomb potentials as follows. Combined with the usual $V \sim 1/r$ outside the nucleus, we get a potential as shown in figure 4.2.

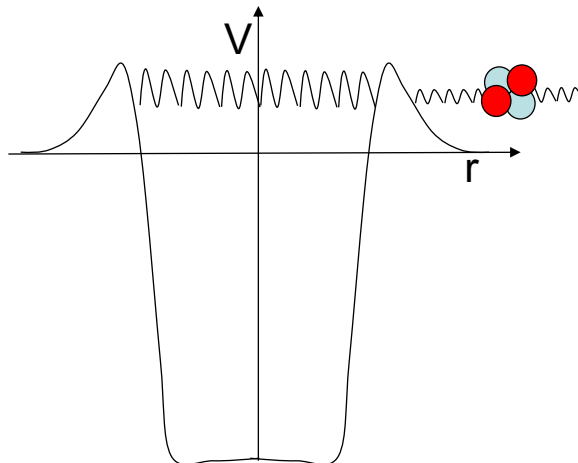
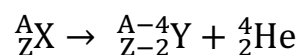


Figure 4.2. Combined nuclear and Coulomb potential well, showing barriers to α -particle escape.

For a combination of a highly bound ^4He nucleus and the daughter nucleus, the total binding can be higher than for the parent nucleus and we reach the condition in figure 4.2b, where the α -particle can escape with excess kinetic energy. That is to say, for;



we have $Q > 0$. Conservation of momentum means that the kinetic energy is mostly taken up by the α particle. However, the kinetic energy is not enough to overcome the potential barrier (see figure 4.2b) and, as we see, quantum tunnelling through the barrier is needed to allow escape of the α -particle. In the following we will derive a formula that tells us the relationship between the kinetic energy of the α -particle and the rate of decay.

First, let us look at a simple quantum barrier as in figure 4.3. We know from PHY2001 quantum

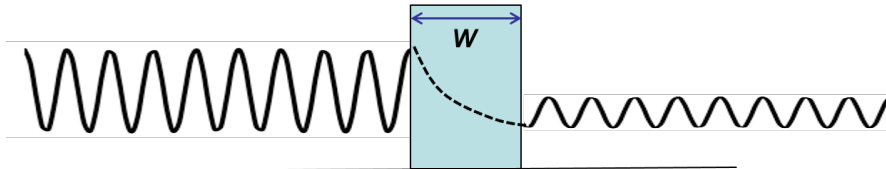


Figure 4.3 A schematic of a simple potential barrier of width w and with a particle incident from left to right.

mechanics that the probability of transmission depends on the ratio of the squares of the wavefunction either side of the barrier, given by;

$$P = \frac{|\psi(w)|^2}{|\psi(0)|^2} = e^{-2\gamma} \quad (4.6)$$

where we assume the barrier starts at $r=0$. The factor, γ is given by

$$\gamma = w \sqrt{\frac{2m}{\hbar^2} (V(r) - K)} \quad (4.7)$$

where m is the mass of the particle and K is kinetic energy. In the square barrier case $V(r)$ is a constant. If we treat the potential barrier in figure 4.2b as a series of square barriers of width dr , we can integrate from the point away from where the barrier starts, R_B , to the point of exit, R_E which is where the kinetic energy matches the potential. Thus

$$\gamma = \int_{R_B}^{R_E} \sqrt{\frac{2m}{\hbar^2} (V(r) - K)} dr \quad (4.8)$$

Let us make some approximations that will turn out to be justified. Firstly, R_E tends to be of order 30-60 fm and so, since the barrier starts more or less where the nuclear potential goes to zero, close to the nuclear radius then, $R_E \gg R_B$. We also note that for the most significant contribution to γ we have $V(r) \gg K$ and we just integrate over $V(r)$ but we then equate the kinetic energy to the Coulomb potential at R_E and make the classical approximation that $K = mv^2/2$ and obtain

$$\gamma = \frac{8Ze^2}{4\pi\epsilon_0\hbar v} \quad (4.9)$$

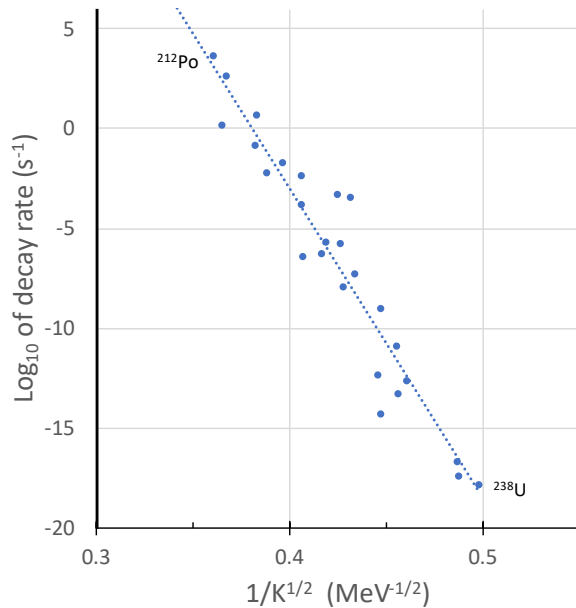


Figure 4.4 (Adapted from Eisberg and Resnick). A plot of known alpha decay rates against the $1/K^{1/2}$ showing broad agreement with the Geiger-Nuttall relation.

where Ze is the charge of the daughter nucleus. Now, the α particles may not penetrate on the first collision (in fact it is unlikely as we shall see). However, they do reflect then and reach the opposite side. We can make a semi-classical estimate of how often they do this. Let us take a typical $K=5$ MeV and a nuclear radius of ~ 7 fm for a heavy element. This implies a classical v of 1.5×10^7 m/s and that means $\sim 10^{21}$ collisions per second. The lifetime expected is then given by

$$\frac{1}{\tau} \sim 10^{21} e^{-2\gamma} \quad (4.10)$$

Now, we can get an idea of the sensitivity by considering an element with say $Z=100$ (look it up to get its name!). For a 5 MeV α particle the value of $\gamma \sim 105$ but for a 10 MeV α particle we would have $\gamma \sim 75$, in

equation 4.9, this would make 26 orders of magnitude difference in the rate of decay, $\lambda = 1/\tau$. If we restate 4.10 in log terms we get

$$\ln(\lambda) = \ln(10^{21}) - 2\gamma \quad (4.11)$$

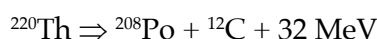
Replacing some constants with A_0 and B_0 and expressing the velocity, v in terms of K , we arrive at the Geiger-Nuttall relationship

$$\ln(\lambda) = A_0 - \frac{B_0 Z}{K^{1/2}} \quad (4.12)$$

In figure 4.4 we can see a plot of many typical cases plotted against the Geiger-Nuttall scaling predicted in equation 4.12. We can understand this behaviour from two points of view. If we look at figure 4.5, we see that for a decay with kinetic energy K_1 the difference between barrier height and potential is smaller than for the lower energy K_2 , meaning that the approximation that $V(r) \gg K$ becomes less valid and we see in equation 4.8 that γ becomes smaller. We also see that the distance that has to be tunnelled though is smaller and thus the integral is also then smaller.

Decay of heavier particles

For other particles like ^{12}C which is also relatively stable, we also expect there to be decay that is energetically favourable. For example;



should be energetically favoured with a Q of +32 MeV. However, several factors work against this. Firstly, the potential barrier to be overcome is higher since the ^{12}C nucleus has a higher charge. This increases γ and the decay is exponentially dependent on this. Also the ^{12}C nucleus is heavier and this also increases γ as can be seen in equation 4.8, although it manifests itself through a lower velocity in equation 4.9. However, decays like this have been seen but with very low rates. We might then ask, why do we not see emission of other small species and nuclei? This is because the particular stability associated with forming a ^4He nucleus makes this a special case. In table 4.1 below, we show how the Q value for decay of ^{232}U varies depending on the species emitted. We see that it is negative for all but the α -decay case.

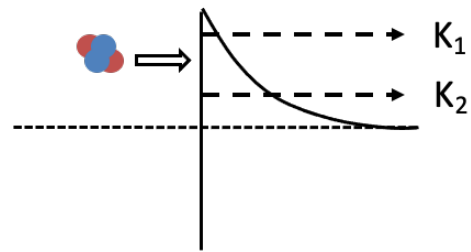


Figure 4.5 Detail of barrier penetration for an α -particle

***a*-decay spectra**

For α -decay, we generally see a fixed energy as we transition, generally from a ground state of a nucleus to a specific state of the daughter nucleus and so each α -particle has the same kinetic energy. However, the daughter nucleus can have many possible end states. In figure 4.6 we see a spectrum from the decay of ^{251}Fm .

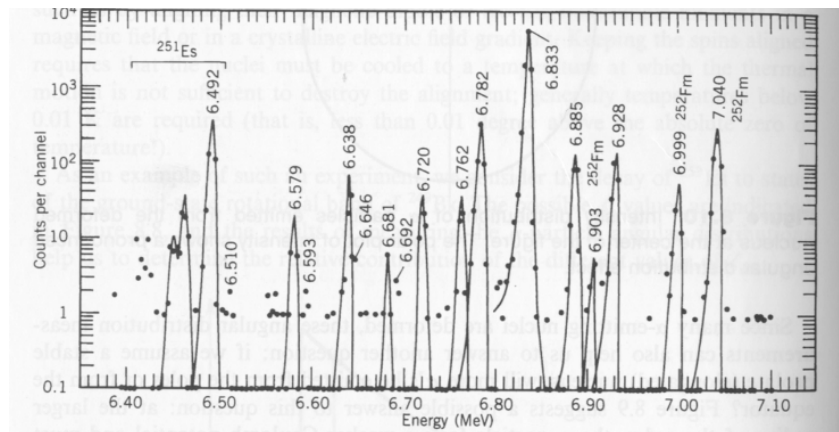


Figure 4.6 α -particle decay spectrum from ^{251}Fm .

Table 4.1 Q values for emission of different nuclear species from ^{232}U

| Emitted Particle | Q value (MeV) |
|------------------|---------------|
| n | -7.26 |
| ^1H | -6.12 |
| ^2H | -10.70 |
| ^3H | -10.24 |
| ^3He | -9.92 |
| ^4He | +5.41 |
| ^5He | -2.59 |
| ^6Li | -6.19 |
| ^7Li | -1.94 |

The spectrum is listed in table 4.2. Notice how the α -particle energies are known quite accurately but also that there is a difference between the particle energy and the transition energy. This is because a small amount of energy is taken up in recoil of the nucleus.

Table 4.2 table of α -decays from ^{251}Fm .

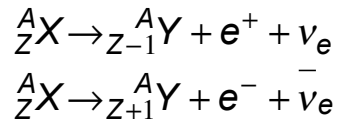
| α group | α energy(keV) | Decay Energy (keV) | Excited state (keV) | α intensity (%) |
|----------------|----------------------|--------------------|---------------------|------------------------|
| α_1 | 7305 \pm 3 | 7423 | 0 | 1.5 |
| α_2 | 7251 \pm 3 | 7368 | 55 | .93 |
| α_3 | 7184 \pm 3 | 7300 | 123 | .29 |
| α_4 | 7106 \pm 5 | 7221 | 202 | \sim 0.05 |
| α_5 | 6928 \pm 2 | 7040 | 383 | 1.8 |
| α_6 | 6885 \pm 2 | 6996 | 427 | 1.7 |
| α_7 | 6833 \pm 2 | 6944 | 479 | 87 |
| α_8 | 6782 \pm 2 | 6892 | 531 | 4.8 |
| α_9 | 6762 \pm 3 | 6872 | 552 | .38 |
| α_{10} | 6720 \pm 3 | 6829 | 594 | .44 |
| α_{11} | 6681 \pm 4 | 6789 | 634 | .07 |
| α_{12} | 6638 \pm 3 | 6745 | 678 | .56 |
| α_{13} | 6579 \pm 3 | 6686 | 738 | .26 |

Applications

In the lectures we will discuss an application of α -particle sources relating to non-destructive testing. Slides will be available for this after the lecture. You can insert a page in your notes here to cover this material.

4.2 Beta decay

In β -decay, if we ignore electron capture (EC) for now, we have two processes to consider;



These are β^+ and β^- decays. In the first, a positron and a neutrino are emitted when a proton is turned into a neutron inside the nucleus. In the second, an electron and anti-neutrino are emitted as a neutron is turned into a proton. The (anti)neutrino has no charge and an extremely small (but finite) mass and does not interact easily and is hard to detect. It has spin $\frac{1}{2}$ like the electron or positron. As with α -decay, the Q-value of the reaction is fixed as we decay from a fixed nuclear state to a fixed, possibly excited, nuclear state of the daughter nucleus. The emission of two particles means that the energy is shared and we measure a spectrum of energies for the electron or positron emitted. We do not change the atomic mass number, A of the parent nucleus but we do change Z.

Q value of the decay

In chapter 1, we discussed binding energy. During a nuclear reaction the binding energy of the particles involved might change and binding changes released as kinetic energy. Consider the total energy to be mass energy and kinetic energy. Let us recall energy conservation for a system that has initial and final mass and kinetic energy and may start in a ground state but may end in an excited state.

$$K_i + M_i c^2 = K_f + M_f c^2 + E_{ex} \quad (4.13)$$

Now, we can define the Q value as the amount of kinetic energy released and for us this is $K_f - K_i$. Re-arranging equation 4.13 and assuming we end in a ground state so that $E_{ex} = 0$, we can see that we can also express Q as

$$Q = K_f - K_i = M_i c^2 - M_f c^2 \quad (4.14)$$

For a ground state to ground state transition this can be called Q_0 and so if we end in an excited state we have

$$Q = Q_0 - E_{ex} \quad (4.15)$$

which makes sense as, if we have an excited state, then less energy is available to go into kinetic energy.

For β -decay we start from this to calculate Q. Now for the process of β^+ decay we can look at the nuclei on each side and the particles emitted- assume for now the ground states only. From the process shown above we can write, assuming the nuclear masses

$$Q_{\beta^+} = (M_{nuc}^{A,Z} - M_{nuc}^{A,Z-1} - m_e - m_{\nu})c^2 \quad (4.16)$$

where we take the positron mass as identical to the electron mass. We shall also assume the neutrino mass to be zero as it is negligible for our purposes. It happens that what is measured

most accurately is the atomic masses of elements- the neutral element in the ground state is known to several decimal places. If we neglect the electron binding energy we can replace

$$M_{at}^{A,Z} = M_{nuc}^{A,Z} + Zm_e \quad (4.17)$$

substituting this into equation 4.16 for the initial and final species we can see

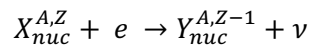
$$Q_{\beta^+} = (M_{at}^{A,Z} - M_{at}^{A,Z-1} - 2m_e)c^2 \quad (4.18)$$

The electron binding energy for the initial and final atomic species are very similar and so the difference between them is small and generally neglected in all the most detailed measurements. In a similar manner, **you** can derive

$$Q_{\beta^-} = (M_{at}^{A,Z} - M_{at}^{A,Z+1})c^2 \quad (4.19)$$

Electron capture

An alternative process is one in which an atomic electron is captured from orbit and we have



By, again, neglecting binding energy and the neutrino mass, **you** can also show that

$$Q_{EC} = (M_{at}^{A,Z} - M_{at}^{A,Z-1})c^2 \quad (4.20)$$

We need the Q values to be positive for these reaction to occur. If β^+ can occur so can EC but not necessarily the other way around as there is ~1.02 MeV difference in required mass difference between parent and daughter nuclei. This latter is for example how Fe⁵⁵ comes to emit 5.9 keV radiation- the gap left in the K-shell is filled by Mn K- α radiation. The figure below shows some examples of decays between C, N and O.

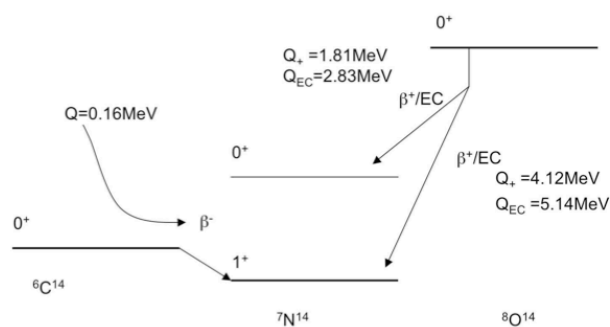


Figure 4.7 Examples of β decay from lower and higher Z isotopes of same atomic mass A.

Spread of electron/positron energy

As noted above, the sharing of the released energy between two particles means that if we measure the kinetic energy of the electron or positron, we get spectra similar to those in figure 4.8.

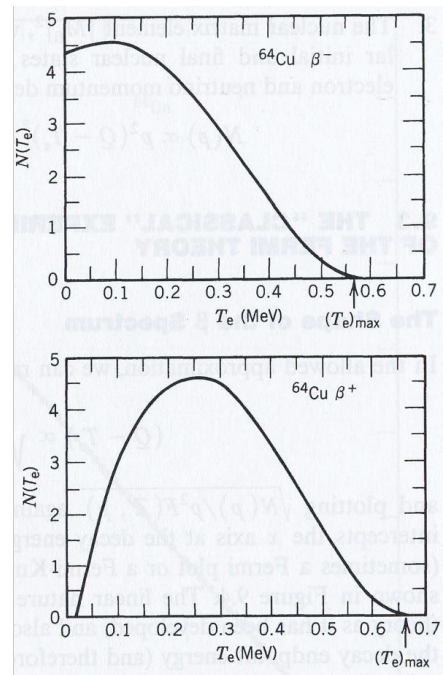


Figure 4.8 Energy spread of β^+ and β^- decay. $N(T)$ is the number detected as a function of kinetic energy, T . Both decays are possible from the parent ^{64}Cu nucleus.

In both cases, we see that the spectrum goes to zero at some maximum value, which is given by the Q of the reaction. It means that in those cases all the energy is taken up by the positron or electron. In both cases the spectrum has a peak somewhere in the middle, except that for the β^+ case it is generally pushed to a higher energy. This is due to the interaction with the nucleus, which is positive and pushes the positron away, whilst for an electron it would tend to pull it back.

For now, we can get a broad understanding of this distribution by considering what we call the density of states. What we mean by this is that if there are more potential final states for a particle with a given energy, then that decay is more likely. Consider the case of β^- decay; for the β^- -particle with momentum p

$$E^2 = p^2c^2 + m_e^2c^4 \quad (4.21)$$

Whilst for the (assumed massless) anti-neutrino with momentum, p_ν

$$E_\nu = p_\nu c \quad (4.22)$$

The total energy emitted is $E_0 = E + E_\nu$, some of which is mass energy for the β^- -particle, $E_0 = Q + m_e c^2$. Now consider that for a decay where the electron takes up a specific momentum, the number of available states of momentum is proportional to the volume in momentum space between p and $p + dp$ and is thus $4\pi p^2 dp$ and a similar argument goes for the anti-neutrino. The number of decays, dN per minute in a sample where the energy is divided between the two particles, scales as;

$$dN \propto 16\pi^2 p^2 p_\nu^2 dp dp_\nu \delta(E + E_\nu - E_0) \quad (4.23)$$

where the delta function ensures conservation of energy. Now realising that the neutrino energy all kinetic and that the total kinetic energy released is Q , and taking the previous equations relating E and p , we can put the neutrino momentum as ;

$$p_\nu = (Q - T_e)/c \quad (4.24)$$

$$dp_\nu = dE_\nu \quad (4.25)$$

$$EdE = c^2 p dp \quad (4.26)$$

We can then see that

$$dN \propto p^2 dp (Q - T_e) \delta(E + E_\nu - E_0) \quad (4.27)$$

We can see from our expression above, that as kinetic energy, T_e tends to zero then the number of particles is expected to go to zero. Likewise as we tend to Q then the term in brackets tends to zero and we also get no particles above this energy. Thus we expect a curve that maximises in the middle as those in figure 4.8 do. This simple analysis does not account for the Coulomb interaction.

Beta decay and angular momentum

Consider the following: If a β -particle is emitted with momentum p from a nucleon at a distance r from the centre of the nucleus, then it imparts an angular momentum $L = \mathbf{r} \times \mathbf{p}$ on the nucleus. In QM we know that, to be non-zero, this must have a minimum numerical value of $\sqrt{\ell(\ell+1)}\hbar$ where $\ell = 1$. This means;

$$L \sim 1.5 \times 10^{-34} \text{ kgm}^2\text{s}^{-1} \sim \mathbf{r} \times \mathbf{p} \quad (4.28)$$

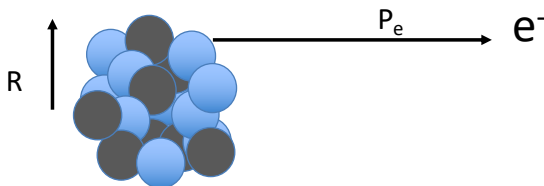


Figure 4.9 Illustrating expected angular momentum transfer with classical mechanics.

Now for a typical case, as seen, for example, in Krane we have $p \sim 1\text{MeV}/c \sim 5 \times 10^{-22} \text{ kgms}^{-1}$. This means that;

$$r \sim L/p \sim 1.5 \times 10^{-34} / 5 \times 10^{-22} \sim 225 \text{ fm}$$

This is way outside the dense part of the nucleus and so we conclude that generally no angular momentum is exchanged. This

leads to the notation that $\Delta L=0$ transitions are called "allowed" and the $\Delta L=1,2,\dots$ are the first and second etc *forbidden* transitions and do occur due to the extended wave nature of the electrons but are 10-1000 times weaker.

Another way to view this is if we take a typical nuclear radius of say ~ 5 fm and calculate the angular momentum imparted by the typical β -particle noted above and emitted from the edge of the nucleus, it has a maximum of $L \sim 2.5 \times 10^{-36} \text{ Kgms}^{-1}$ which is well below the quantum unit.

Selection rules

The emitted particles, electrons or positrons and anti-neutrinos and neutrinos have spin $1/2$. If these are opposite to each other, then the spin carried off is $S = 0$ and we have *Fermi* decay. For spins aligned then $S=1$ is carried off and we have a *Gamow-Teller* decay. The total nuclear spin of the system is then

$$\mathbf{J}_p = \mathbf{J}_d + \mathbf{L} + \mathbf{S} \quad (4.29)$$

where 'p' and 'd' refer to the parent and daughter nucleus and L is the orbital angular momentum carried off by the electron-neutrino pair. Now, we have determined that for allowed transitions, no orbital angular momentum can be carried off and so $L = 0$. Thus, for the *Fermi case*, with $S=0$, the change in nuclear spin can only be zero. For the *Gamow-Teller case*, we have $S=1$ and vector addition of these angular momentum vectors means that we can have $\Delta J=0, \pm 1$ although $\Delta J=0$ will not work for both $\mathbf{J}_p = 0$ and $\mathbf{J}_d = 0$ since it depends on re-orientation of vectors to allow for no change whilst carrying off $S=1$ angular momentum and that cannot occur for zero length vectors. Such transitions are, therefore, purely Fermi. Since we do not change angular momentum, we can say that parity (Chapter 1) does not change and so $\Delta P=0$ as well. In summary, selection rules for allowed transitions are;

$$\begin{array}{ll} \Delta L=0 & \\ \Delta J=0 & \text{Fermi} \\ \Delta J=0, \pm 1 & \text{Gamow-Teller} \\ \Delta P=0 & \end{array}$$

Isobar stability curves

In chapter 1 and in chapter 3, we discussed the idea that stability of nuclei depends on a particular ratio of neutrons to protons that changes according to the atomic mass number, A. Let's discuss this in terms of stability to β -decay. Look at figure 4.10, which is a Segré chart with an arrow cut across at 90° to the $N = Z$ line. This arrow traverses a constant A value. For isotopes above the line of stability (black squares) we have an excess of protons and there is instability to β^+ -decay, meaning that it is energetically favourable ($Q > 0$) to undergo this transition. Likewise for isotopes below the line of stability, there is an excess of neutrons and β^- -decay is favourable.

In figure 4.11 we show two of these isobars, one for an even A and one for an odd. The figures show the mass energy of the isotope. we can see that there appears to be very little difference, but the differences are in MeV of energy and thus this is the typical decay energy. Notice, how there is a particular isotope that has the lowest mass and the others are unstable to β -decay or electron capture.

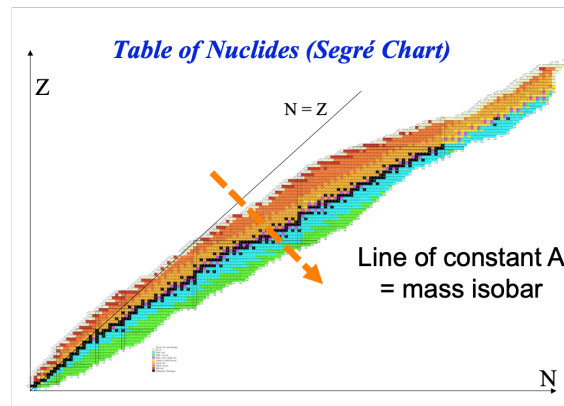


Figure 4.10 Segré chart of elements. The ones in black are stable isotopes. The dashed arrow shows a line of constant atomic mass number, A , because it is at right angles to the $N=Z$ line.

For the case of $A=128$ note how there are effectively 2 curves. This is because we can have either an even-even nucleus or odd-odd. We noted earlier that odd-odd is not so stable as even-even due to the pairing effect (see Chapter 3). This creates an interesting situation regarding ^{128}Te and ^{128}Xe . We can see that ^{128}Xe is more stable. However, in order to reach it, a sample of ^{128}Te would first have to decay to ^{128}I , which requires a $Q < 0$ and is thus not likely. The possibility of a double β -decay directly to ^{128}Xe has been explored and is an important experiment in particle physics, but it is well beyond undergraduate physics to discuss this.

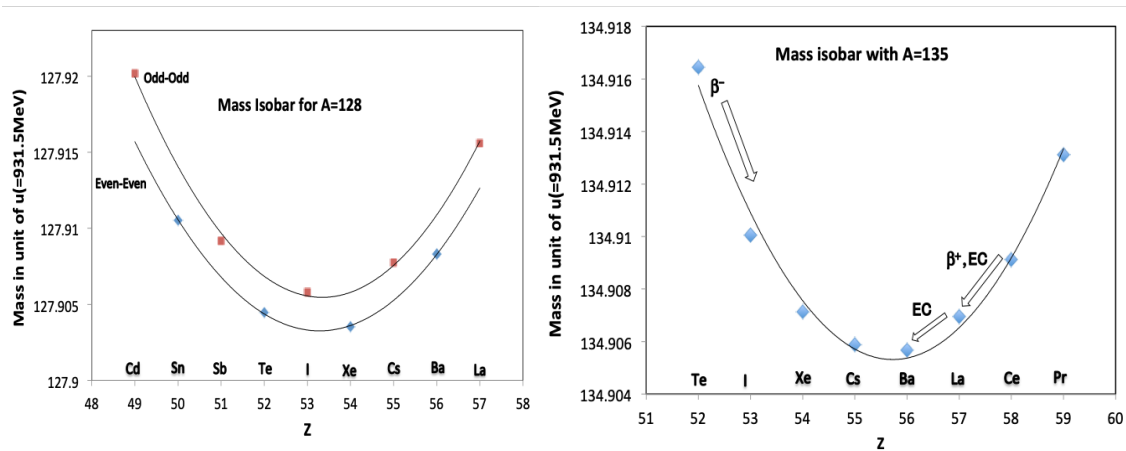


Figure 4.11 Mass isobars for both even and odd atomic mass.

Applications

As with α -decay, we will discuss some important applications of β -decay in the lectures and make the slides available after the lectures.

4.3 Gamma-decay

If we bombard a nucleus with energetic particles, we can excite it to higher energy levels. For example, in figure 4.12 we see the result of bombarding ^{27}Al with 5 MeV protons. We generate a spectrum of gamma rays that is due to relaxation from upper to lower levels. By analysing the spectra we can reconstruct the nuclear energy levels. This is a powerful tool in measuring the energy levels of nuclei so that they can be compared to models such as those outlined in chapter 3.

Quadrupoles and dipoles

In atomic physics, you will have seen that there are selection rules for emission. The emission from atoms is predominately dipole emission. That is, in classical terms, we can consider the

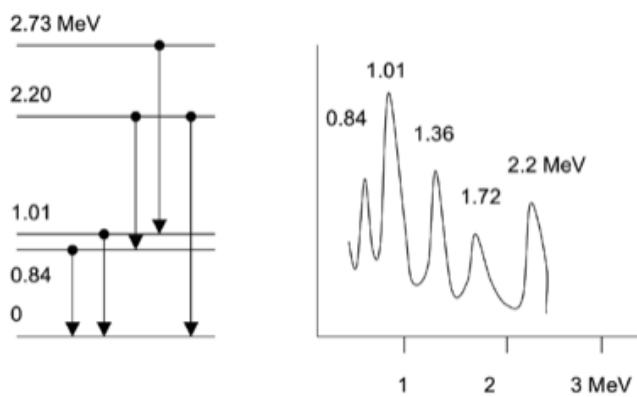


Figure 4.12 On the left are the energy levels for ^{27}Al . On the right is schematic spectrum of gamma rays emitted after bombardment with energetic protons of 5 MeV kinetic energy (Krane).

electron undergoing a transition in an atom as an oscillating charge, you should come across this in more detail in EM courses. In quantum mechanics this is expressed in terms of a dipole operator, \mathbf{er} operating between the initial and final states:

$$\int \psi_f^* \mathbf{er} \psi_i d^3r$$

Where the integral is over volume, e is the charge unit and \mathbf{r} is the position operator. The intensity of emission is given by the square of this matrix element. It emerges that there are

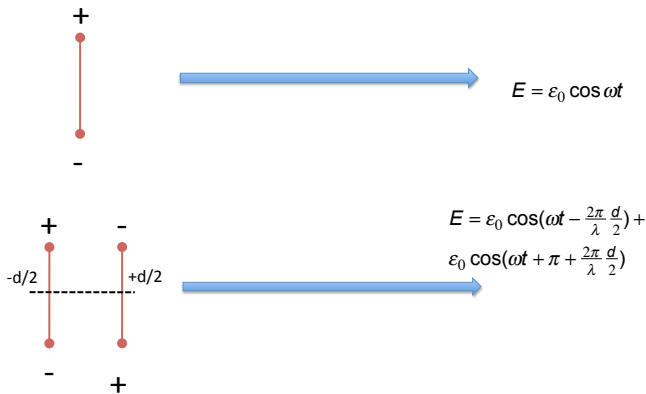
other forms of radiation, for example quadrupole emission. The discussion below will help explain why this is small in atomic physics but significant in nuclear physics. We know that for an oscillating dipole- a charge oscillating back and forth is accelerating and we know that this produces radiation. This is maximised normal to the direction of oscillation of the charge. At some distance away, we can assume that the electric field of the radiation given off is given by:

$$E = E_0 \cos(\omega t) \quad (4.30)$$

Now look at figure 4.13 where we place two dipoles side by side. (we can think of the + charge as being the nucleus at rest and an electron is oscillating if you like). We assume that the two dipoles work in anti-phase, that is the oscillations are out of step with each other so that the total dipole moment is zero. However, this arrangement, with a finite separation, d , between dipoles constitutes a quadrupole and we can estimate the field seen as a result of adding the two fields from the dipoles. Clearly from the figure there is a phase difference. The total field is given by:

$$E = E_0 \cos\left(\omega t - \frac{2\pi d}{\lambda}\right) + E_0 \cos\left(\omega t + \pi + \frac{2\pi d}{\lambda}\right) \quad (4.31)$$

where we have accounted not just for the path difference but also that the dipoles are 180° out of phase with each other (the π in the second term). It turns out quite simply that this can be re-written as;



$$E = 2E_0 \sin\left(\frac{\pi d}{\lambda}\right) \sin(\omega t) \quad (4.32)$$

Figure 4.13 arrangement of two dipoles to form a quadrupole.

where λ is the wavelength of the light emitted. So now, we can compare the intensity of light given off by a quadrupole to that for a dipole. Comparing the dipole field and the field above, we can see that the amplitude ratio is given by;

$$2 \sin\left(\frac{\pi d}{\lambda}\right)$$

Now, for an atom, the wavelength is about 5000 Å for optical radiation but the atom is only about 1 Å in size. This means the ratio of quadrupole to dipole is

$$2 \sin\left(\frac{\pi d}{\lambda}\right) \sim 10^{-3}$$

This the amplitude ratio and the intensity is given by the square of the amplitude so the ratio of intensity is more like 10^{-6} . Thus quadrupole emission is usually unimportant for atoms.

Now consider a nucleus. A gamma ray from Al has energy 1 MeV for one of the transitions above. This corresponds to 0.0124 Å. The size of the nucleus is ~7 fm. Thus the ratio $2 \sin(\pi d/\lambda) \sim 0.035$ and so, in intensity terms, quadrupole emission is ~ 1000 times more important than for the atomic case. For heavier nuclei and higher energy transitions we can see this trend would be even stronger.

Magnetic Dipole Emission

Electromagnetic theory tells us that electric dipole radiation depends on oscillating charges. For magnetic emission, it depends on oscillating currents. For magnetic dipoles, electromagnetic theory shows that the emission ratio between magnetic dipole and electric dipole radiation is

$$\left(\frac{\mu}{pc}\right)^2$$

where p is the electric dipole moment that we approximate as $p \sim eR$ where R is the nuclear radius and e is the proton charge. We have μ , the magnetic dipole. For a loop of charge this is

$$\mu = IA \quad (4.33)$$

where the area is $A = \pi R^2$ and the current is $I = ev/2\pi R$. Thus, we can show that the ratio of magnetic to electric dipole radiation is proportional to $(v/c)^2$. For a typical value of $R \sim 5$ fm this works out at a ratio of $\sim 1/80$ because the charges move at $\sim 10^7$ ms⁻¹. This ratio is about 10-100 times larger than seen in atomic physics and thus magnetic emission is more important in nuclear physics than atomic physics.

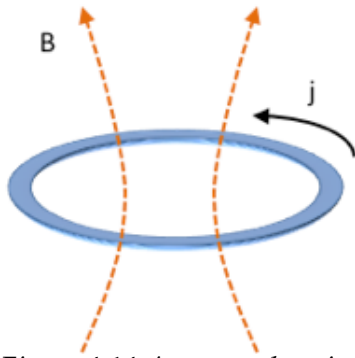


Figure 4.14 A current loop in the nucleus leads to a magnetic field which, if oscillating gives magnetic radiation.

Selection rules

The selection rules that are relevant depend on the pole in question. For dipole radiation the matrix element between the initial and final state eigen-functions is simply $e\mathbf{r}$ where e is charge and \mathbf{r} is spatial position. It is because this is asymmetric with respect to co-ordinates that the initial and final state have to have opposite parity (see atomic notes). We have;

$$\Delta J = 0, \pm 1 \quad (\text{but not } J=0 \text{ to } J=0)$$

$$\Delta P = 1 \quad (\text{Yes), i.e. the parity changes}$$

The photon has intrinsically spin 1 hence the need to change either the value or the orientation of J , the nuclear spin. For a magnetic dipole emission the relevant matrix element μ the magnetic moment. As you saw in atomic physics, this scales as $\sim \mathbf{r} \times \mathbf{p}$ since it is proportional to angular momentum. This has even parity as reversing the directions of both \mathbf{r} to $-\mathbf{r}$ and \mathbf{p} to $-\mathbf{p}$ does not introduce a net negative sign and thus has even parity. The selection rules are now;

$$\Delta J = 0, \pm 1 \quad (\text{but not } J=0 \text{ to } J=0)$$

$$\Delta P = 0 \quad (\text{No})$$

For a quadrupole (see discussion of quadrupole in Chapter 1) we have an operator with a spatial part $\sim 3z^2 - r^2$ and is even parity. This is corresponding to a photon with $L=2$ angular momentum- this includes intrinsic spin and angular momentum relative to the nucleus (possible since we no longer have an effective point source)- and even parity and so the selection rules are;

$$\Delta J = 0, \pm 1, \pm 2 \quad (\text{but not } 0 \rightarrow 0 \text{ or } 0 \rightarrow 1, 1 \rightarrow 0 \text{ or } 1/2 \rightarrow 1/2)$$

$$\Delta P = 0 \quad (\text{No})$$

Some typical transitions are shown in figure 4.15.

For a typical $A \sim 100$ the gamma decay lifetimes depend a lot on the energy of the gamma ray and typically vary from 10^{-10} - 10^{-20} s for M5 (high order magnetic) radiation but from 10^{-10} to 10^{-15} s for electric dipole radiation



Figure 4.15 Some typical transitions resulting in gamma radiation. We have seen that magnetic dipole (M1) and electric quadrupole (E2) emission is quite likely in nuclei.

Internal conversion

This process competes with gamma emission. Instead of decaying to a lower state by emission of a gamma ray, a nucleus decays by transferring energy to an atomic electron. It is a one-step process that does not involve the emission of a gamma ray followed by absorption by the electron. The kinetic energy of the electron is

$$K_e = \Delta E - B \quad (4.33)$$

where B is the binding energy and ΔE is the transition energy. In figure 4.16 we see an example of this. In this case, ^{203}Hg has decayed by β -decay to an excited state of ^{203}Tl . Now, the ^{203}Tl can decay to the ground state by γ -emission but as we see in figure 4.14 there is also a spectrum of emitted electrons created by internal conversion. The upper figure gives a broad spectrum showing peaks corresponding to the different shells. The energies are given by the 279.19 KeV of the excited state minus the energy needed to free the electrons from the K,L, M etc shells. The energies are thus

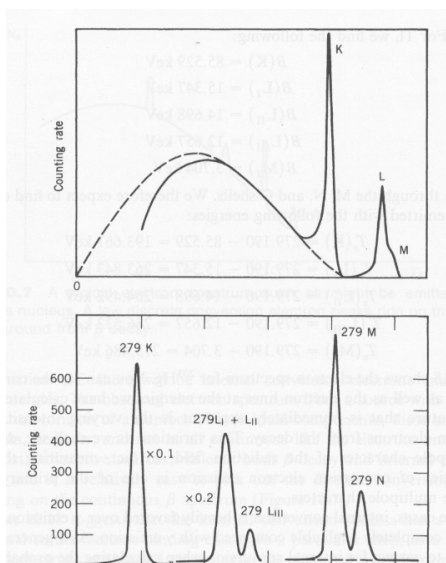


Figure 4.16 Electron spectra from ^{203}Tl nuclei decaying by internal conversion. Top: Broad spectrum, bottom: detailed spectrum.

$$K_e(K) = 279.190 - 85.529 = 193.661 \text{ keV}$$

$$K_e(L_i) = 279.190 - 15.347 = 263.843 \text{ keV}$$

$$K_e(L_{ii}) = 279.190 - 14.698 = 264.492 \text{ keV}$$

$$K_e(L_{iii}) = 279.190 - 12.657 = 266.533 \text{ keV}$$

The study of these spectra can reveal a lot of information about the nuclear transitions but this is beyond this course.

Emission Recoil

When a γ -ray is emitted from a nucleus it can have a great deal of momentum, depending on the energy of the photon, $p = E/c$. In order to conserve momentum, the nucleus must recoil and thus take up both momentum and energy. The recoil momentum is of course the momentum of the photon and the recoils energy, in the classical limit (usually valid in this context), is $p^2/2M$ where M is the mass of the nucleus. Thus for an initial and final nuclear state, we have for energy and momentum conservation

$$E_i = E_f + E_\gamma + K_{recoil} \quad (4.34)$$

$$0 = P_{recoil} + P_\gamma \quad (4.35)$$

Now, we know how energy and momentum are related for the photon and for $\Delta E = E_i - E_f$ we get

$$\Delta E = E_\gamma + \frac{E_\gamma^2}{2Mc^2} \quad (4.36)$$

where M is the mass of the recoiling atom. Let us consider, for example ^{51}Cr which can be created in chromium steel by neutron activation and that it will decay to ^{51}V by β -decay and then emit γ -rays of 320 keV. This will give over 1 eV recoil energy to daughter atoms. This means that the gamma ray emitted does not have quite the energy of the transition it is created from. Furthermore, in order to be re-absorbed by another nucleus, a gamma ray needs to have not only the transition energy but the additional recoil energy created when the momentum of the photon is absorbed. The γ -ray emissions have very narrow width generally (10^{-6} to 10^{-3} eV) and for this reason, creation of a γ -ray laser has not been achieved using nuclear transitions, despite some attempts.

The Mössbauer effect

We can see in figure 4.17 an illustration of how the emitted photon energy and the required energy for absorption are separated by twice the recoil energy. The width of the transitions can be broadened to about 0.1 eV by Doppler broadening if the sample is heated but this means only a small overlap between the emission and absorption profiles.

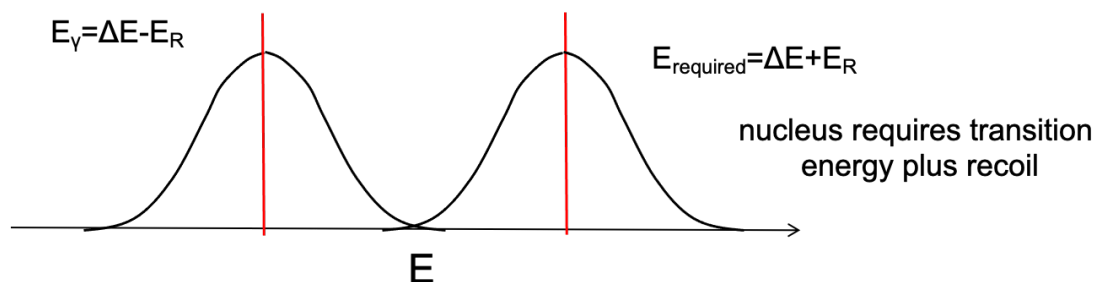


Figure 4.17 A γ -ray emitted from a nucleus gives some energy to recoil of the nucleus, whilst an absorbed nucleus needs to have the transition energy plus the necessary recoil energy.

In 1958 Mössbauer discovered that the recoil could be brought to essentially zero for a cooled sample with modest γ -ray energy. The case he observed was for decay of ^{191}Ir with a photon energy of 129 keV. The recoil energy for the ^{191}Ir atom should be 0.047 eV. This is not enough

to displace the atom and so, since about 10% of atoms were in the lowest vibrational state, the interaction is with the whole lattice rather than a single atom. Thus, since $M_{lattice} \gg M_{Ir}$,

$$\Delta E = E_\gamma + \frac{E_\gamma^2}{2M_{lattice}c^2} \sim E_\gamma \quad (4.37)$$

The transition width is about 3×10^{-6} eV since we have no Doppler broadening due to being in the vibrational ground state. This is about 1 part in 4×10^{13} , a very precise value.

Applications

As with the other decays, we will present some applications in the lectures and make the material available afterwards.

CHAPTER 5: FISSION AND FUSION

5.1 Nuclear Fission

Nuclear fission is a very important process that occurs when a heavy nucleus splits into two lighter ones plus a few neutrons, with a large release of energy. We can see from our earlier chapters (see figure 5.1) that for $A \sim 240$ the binding energy is ~ 7.6 MeV/nucleon whilst for $A \sim 120$ we have ~ 8.5 MeV/nucleon. Thus, we can estimate that if a heavy nucleus splits, we can potentially release ~ 200 MeV.

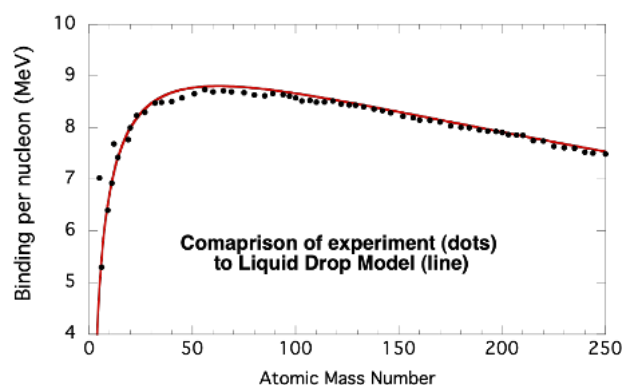


Figure 5.1 Binding energy curve

This means that 1g of fuel, which would contain about 2.5×10^{21} nuclei can generate about 10^{11} J, enough to power a 750 MW power station for two minutes. We can also note from earlier that heavy nuclei tend to have a higher ratio of neutrons to protons than lighter ones. This means that when we create two stable light nuclei from one heavy one, we tend to have an excess of

neutrons. These neutrons are important in inducing further fission decays and instigating a *chain reaction*.

Spontaneous fission can occur if a large nucleus vibrates and stretches in the process. We can see a schematic of this in figure 5.2. We can see that there is a fission energy barrier to be overcome.

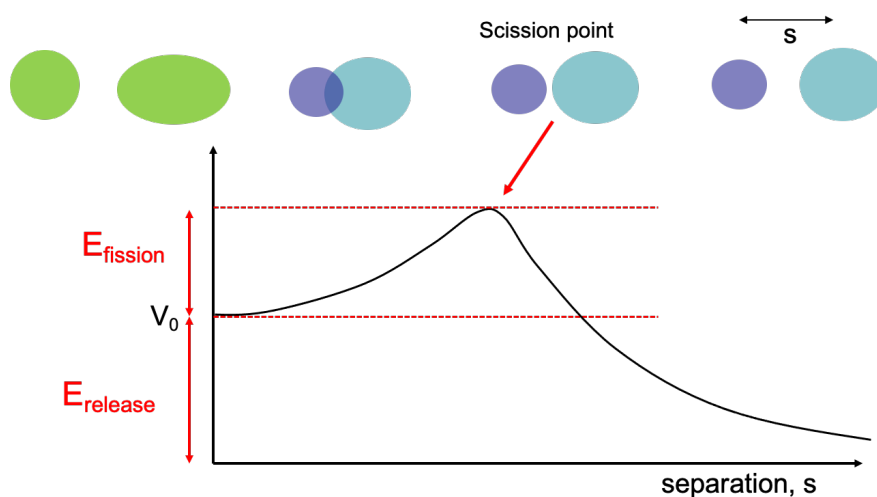


Figure 5.2 Schematic of a fission event. Stretching of the nucleus requires energy as we shall explore in the text. At some separation two products separate enough (scission point) that further separation is energetically favoured because we move from high atomic mass to lower masses closer to the peak of binding energy.

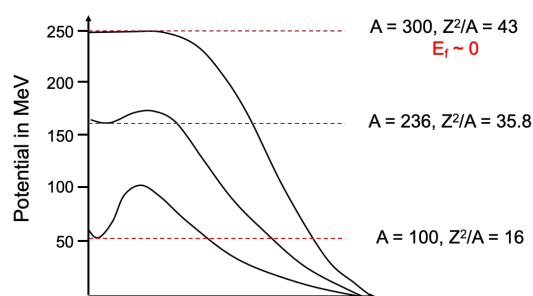


Figure 5.3 Variation of fission barrier with atomic mass, A

For ^{236}U , the fission energy required is ~ 6 MeV, and this usually does not undergo spontaneous fission. Higher mass elements have lower fission energies and do undergo spontaneous fission, helped by the possibility of quantum tunnelling of products through this potential barrier. The likelihood of spontaneous fission by tunnelling of course depends strongly on the size of the barrier and varies from 10^{16} years for ^{238}U to ~ 50 minutes

for ^{256}Fm . In figure 5.3 we see, schematically, how the barrier varies with atomic mass number.

We will try to understand fission in terms of a liquid drop model. Take a spherical nucleus with radius R . In chapter 3, we saw we could develop a model of the binding energy, B . Since the state is bound the potential is negative. Stretch it to an ellipsoid so that the volume is conserved, as nuclear matter is effectively incompressible. It can be shown (not by us) that the semi-axes are now

$$a = R(1 + \varepsilon) \text{ and } b = R(1 + \varepsilon)^{-1/2}$$

The surface energy term in the liquid drop model is increased (to give lower binding) because the surface area increases

$$\text{Area} = 4\pi R^2(1 + \frac{2}{5}\varepsilon^2 + \dots) \quad (5.1)$$

where the ... means higher order terms. The Coulomb term, on the other hand, is decreased by a factor $(1 - \frac{1}{5}\varepsilon^2 + \dots)$, because the proton charges are separated more and so repel less. This increases binding. These effects are competing and the net change in binding energy can be rewritten as

$$\Delta B = B(\varepsilon) - B(0) \quad (5.2)$$

$$\Delta B \approx -a_S A^{2/3}(1 + \frac{2}{5}\varepsilon^2) - a_C \frac{Z^2}{A^{1/3}}(1 - \frac{1}{5}\varepsilon^2) + a_S A^{2/3} + a_C \frac{Z^2}{A^{1/3}} \quad (5.3)$$

$$\Delta B \approx [-\frac{2}{5}a_S A^{2/3} + \frac{1}{5}a_C \frac{Z^2}{A^{1/3}}]\varepsilon^2 \quad (5.4)$$

Now, if the term in square brackets in equation 5.4 is < 0 then the binding energy gets smaller with ε . This means that, as in figure 5.2, the potential gets larger (less negative) with ε and since $F = -\partial V / \partial r$, there will be a restoring force to return to a spherical shape. However, if it is > 0 then as ε increases the binding energy and the nucleus is unstable to fission. This condition arises if

$$\frac{2}{5}a_S A^{2/3} > \frac{1}{5}a_C \frac{Z^2}{A^{1/3}} \quad (5.5)$$

Taking the values of a_s and a_c from Chapter 3, we then arrive at

$$\frac{Z^2}{A} > 47 \quad (5.6)$$

as a condition for instability to spontaneous fission. Now, since at high A we have seen that $Z \sim 0.4A$ this means that we do not expect to have nuclei with A larger than about 300. Of course, this analysis is based on a simple liquid drop model but may help us to understand why there is a limit to the size of nuclei we encounter. For uranium we have $Z^2/A \sim 35$ and so spontaneous fission is not expected. We discuss induced fission next.

Induced fission

We have seen that fission can occur spontaneously by QM tunnelling. However, a very

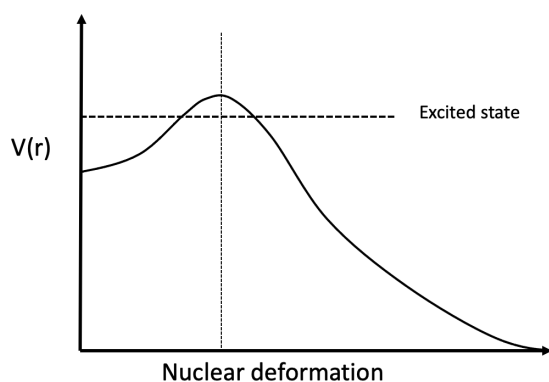
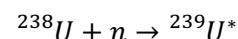


Figure 5.4 capture of a neutron to create an excited state brings the nucleus closer to the potential peak at the scission point.

important type of fission is that induced by capture of a neutron. As the neutron is captured into the nuclear potential well, it releases binding energy that excites the nucleus. We can see in figure 5.4 that this means we have a smaller and narrower effective potential barrier to overcome, and this hugely increases the fission rate. For example for



the neutron capture releases about 5 MeV excitation, reducing the potential barrier from about 6 MeV to ~ 1 MeV. With a high

energy neutron of say 1 MeV energy, the additional kinetic energy can raise the excited state enough to cause fission directly. However, we can also consider the following case

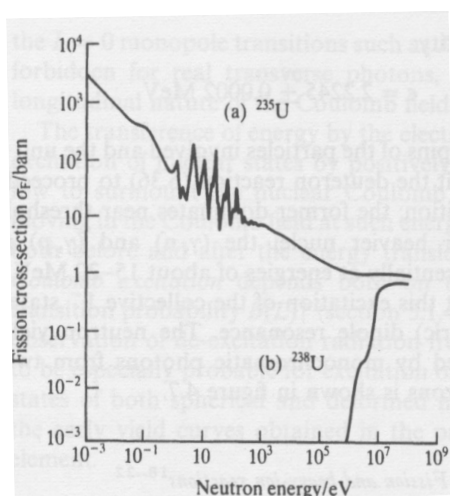
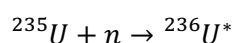


Figure 5.5 cross section for neutron induced fission in uranium.

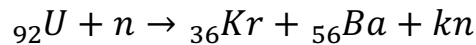
This has an excitation of ~ 6.4 MeV, enough to overcome the barrier directly for a slow neutron with negligible kinetic energy. We can understand this different behaviour by recalling that even-even nuclei are more bound generally and we are creating an even-even nucleus in the latter case. This makes a key difference that can be seen in figure 5.5. The cross-section for fission with slow neutrons is very high for ^{235}U but for ^{238}U we need to have ~ 1 MeV to see a significant cross-section.

The ^{235}U fission cross-section is highest for slow i.e., thermal neutrons (this is related to the large de Broglie length for the particles and can be shown

to have a $1/v$ dependence- not derived here). This is the basis of nuclear fission in a reactor (and of course a bomb). For natural uranium, ^{238}U is the dominant isotope and so enriched uranium with a higher ^{235}U content is often used for nuclear power and certainly for weapons.

Fission products

A typical fission reaction can be



where $k > 1$ and I have deliberately left the atomic mass numbers off, since they will depend on k . There are two things to note. The first is that for $k > 1$ (typically 2-3) we have the possibility of increasing the number of fissions in a chain reaction. The reason for the *spare* neutrons is that in creating new, lower atomic mass, elements, we shift the stable isotopes for these elements to a lower ratio of neutrons to protons than was appropriate to the higher atomic mass parent element (see Chapter 1). The product nuclei are not necessarily in the ground state and a series of decays can then take place as indicated in figure 5.6.

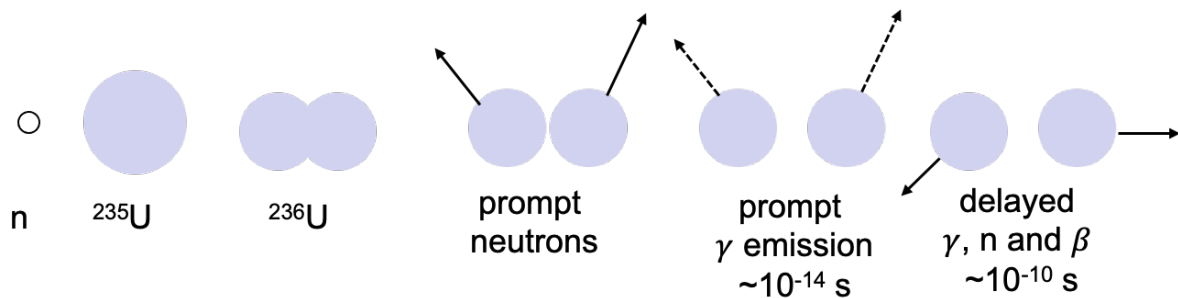


Figure 5.6 Once fission occurs with prompt emission of neutrons, decay to the ground state by γ emission and further delayed neutrons and β particles can occur.

When a heavy nucleus fissions to produce two lighter nuclei, it is rare that the two products are of the same size. In fact, a distribution such as seen in figure 5.7 is seen. We see a strong dip in the middle. The fission products tend to fall around $A \sim 95$ and $A \sim 135$ for example

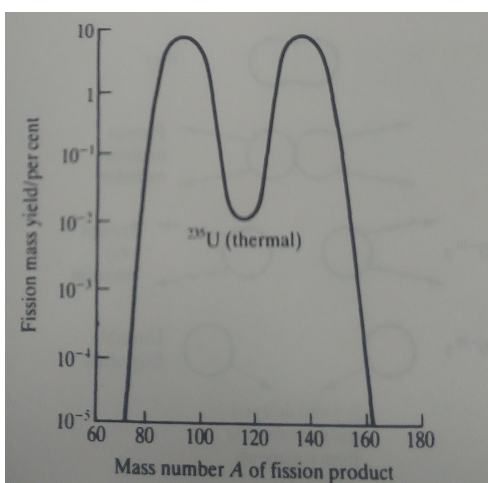
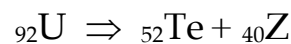


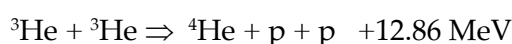
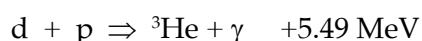
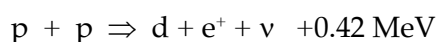
Figure 5.7 typical distribution of fission products



A simple understanding of how this comes about by considering the potential barrier to separation of a fission product and showing that it maximises when the products have the same number of protons.

5.2 Nuclear Fusion

Take another look at figure 5.1. We can see that for heavy elements, there is a release of energy when breaking heavy nuclei apart. For lighter elements, fusing them will generate energy as binding energy is released as kinetic energy. Fusion reactions are what powers the Sun. For hydrogen burning we have several reactions



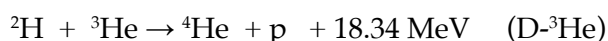
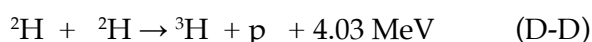
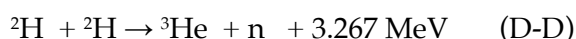
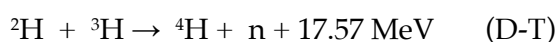
The first reaction involves the weak nuclear force and is quite slow. In addition, the potential barrier to be overcome between the protons is ~ 1 MeV and the mean kinetic energy of the particles at the core of the Sun is ~ 0.001 MeV. However, despite this the Sun produces copious amounts of energy because the matter is contained for a long time (billions of years!) and there is plenty of opportunity for protons at the tail end of the energy distribution to interact.

After the phase where ${}^4\text{He}$ is produced, the next main stage is production of ${}^{12}\text{C}$ via the *triple alpha process*, where three ${}^4\text{He}$ nuclei fuse. After this, heavier and heavier nuclei are formed as the star evolves.

An application: Fusion on Earth

For about 60 years now there has been a significant effort to generate fusion power on Earth. One of the reasons for this is the extremely high yield of energy. For fusion we can generate about 3×10^{14} J per kg of fuel. For fission we have $\sim 2 \times 10^{12}$ J/kg and for coal $\sim 3 \times 10^7$ J/kg. This is a large and complex area of research, and we will only point out some key features and ideas.

There is a problem in simply trying to apply the p-p fusion reaction, as in the Sun. The cross-section is too small, the reaction is very unlikely and only works in the Sun as the material is contained at high density (~ 10 times solid) and collisions are extremely frequent. However, on Earth, we look to reactions with higher cross-section. These include using deuterium (${}^2\text{H}$) and tritium (${}^3\text{H}$) in the so-called D-T reaction. Some possible reactions are



The first of these is the most common, and this can be understood from figure 5.8 which shows the reaction cross-sections of the reactions above and a couple of others as a function of the particle energy. It is clear that the DT reaction is by far the easiest to work with. The peak of the reaction is at $E \sim 0.1$ MeV. However, simply colliding the D and T nuclei together in beams will not work as the Coulomb interaction will simply deflect ions from each other before they

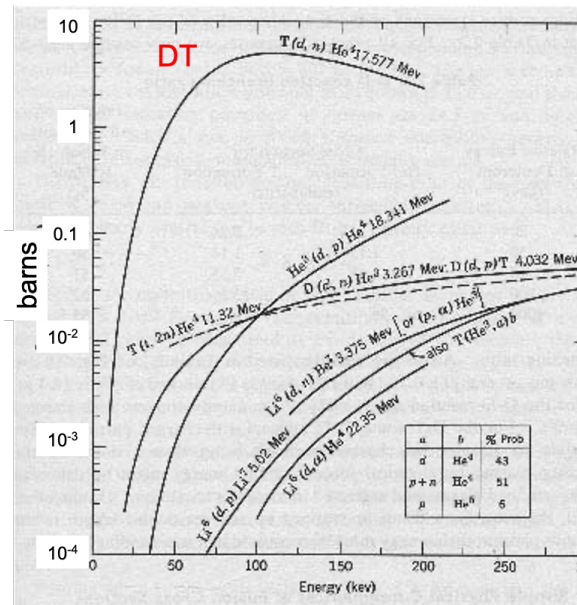


Figure 5.8 Cross-sections for fusion reaction as a function particle energy. The DT reaction is by orders of magnitude the easiest. The cross section is in units of barns = 10^{-24} cm^2 .

can get close enough for short range nuclear forces to come into play that will fuse them. What is needed is to confine them, so that nuclei get many chances to fuse as they collide repeatedly. The Sun does this using gravity as confinement. However, this is not practical on Earth and other ways are found. There are two main approaches.

Magnetic Fusion

If we create a hot plasma (a gas so hot the electrons are ripped from the atoms), then we can contain this within magnetic fields. This is what is attempted in a Tokamak (the word is Russian in origin) is for. We can see that it is basically a toroidal (doughnut shaped) vessel that uses poloidal and toroidal magnetic fields to contain charged particles. This is important as the plasma

needs to be at the optimal temperature of 10^8 - 10^9 K to operate and any contact with the solid vessel will prevent the plasma reaching this temperature range.

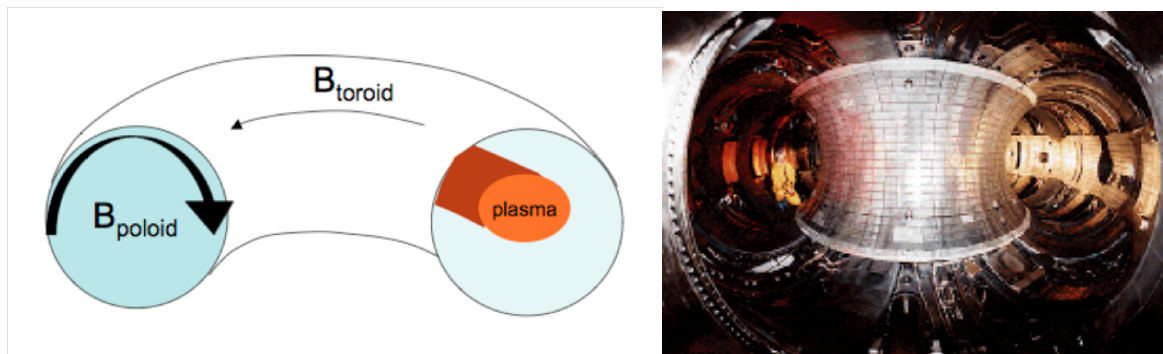


Figure 5.9 Left: A schematic of the inside of a Tokamak. The combination of poloidal and toroidal fields creates field lines that spiral round on themselves and charged particles are constrained to move along these. Right: Photograph of the TTR reactor at Princeton. See the man in yellow hazmat suit for scale.

The question that we need to address is how hot and how dense must the plasma be and how long contained in order to achieve fusion with more energy released than put in to heating the plasma? This question was addressed by Lawson and colleagues. We can see the optimal temperature in figure 5.10. The cross-sections in figure 5.8 have been convolved with a Maxwellian distribution of velocities for a range of temperature and we see that 10^9 K is best for DT fusion. In practice, we operate at $\sim 2 \times 10^8$ K as this is achievable technologically. Lawson calculated that if we have this temperature then we need to also achieve

$$nt > 10^{14} \text{ cm}^{-3}\text{s} \quad (5.7)$$

where n is the density of nuclei in cm^{-3} and t is the confinement time. This is known as the *Lawson criterion*. For typical Tokamaks, n is of order 10^{14} cm^{-3} and so confinement times of order seconds are needed for efficient fusion. This approach is taken at JET and at the ITER reactor being built in Cadarache in France.

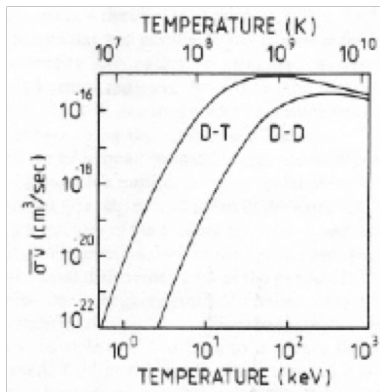


Figure 5.10 Fusion rates for the D-T and D-D reactions

<https://www.iter.org>

Inertial Confinement Fusion

In this approach, we aim only for a very short confinement time but at very high density. The most common approach is to use high power lasers to heat the outer part of a \sim mm sized spherical capsule containing DT fuel. The rapid compression heats the core of the fuel to the point of ignition and then a nuclear burn wave uses up the rest of the fuel, generating about 200 MJ of fusion energy for \sim 1-2 MJ of laser energy.

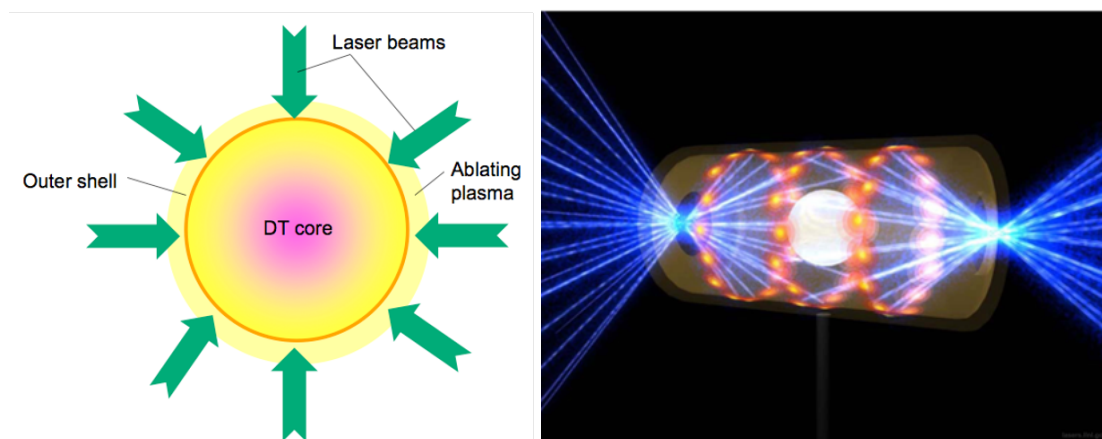


Figure 5.11 Schematic outlines of Left: direct drive fusion and Right: indirect drive

In figure 5.11 we see schematics of two approaches using high power lasers. In *direct drive*, the lasers are incident on a fuel capsule directly. The rapid heating (10^{-9} - 10^{-8} s) of the outer layers creates an inwards reaction as the outer layer streams away (the process is called ablation). This drives a shock that compresses the spherical capsule until the centre reaches ignition temperature of order 10^8 K. The density is intended to reach several hundred gcm^{-3} and the confinement time is of order of picoseconds (10^{-12} s). An alternative is shown on the right in figure 5.11. This is called *indirect drive* and in this, the capsule is contained in a gold-lined cylindrical cannister. The laser beams enter through the cannister ends and illuminate the gold laser- turning it into a hot plasma that emits x-rays with great efficiency. The x-rays heat the outer layer of the capsule and, as with direct drive, the capsule is driven to implode. This latter method has the advantage that the x-ray bath can be made to be more uniform than direct illumination, thus avoiding the severe problems with hydrodynamic instabilities that occur for direct drive. The biggest, experiment so far has been ongoing at National Ignition Facility at the Lawrence Livermore National Laboratory

<https://www.llnl.gov/news/national-ignition-facility-experiment-puts-researchers-threshold-fusion-ignition>

Thus far fusion has not been realised but much progress has been made over the years. An important reason for trying is the potential for much reduced nuclear waste issues with fusion compared to fission. Figure 5.12 shows the expected radioactive waste generated in terms of Curies per Watt of power generated over the lifetime of a reactor. We can see that for fusion over a >10-year period there are significant advantages.

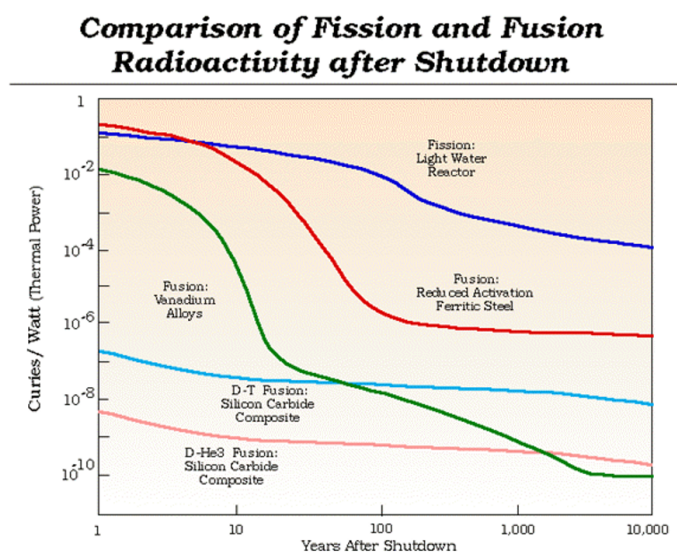


Figure 5.12 Curies of radioactivity per Watt of power generated for different nuclear power schemes.